



## Article

# Bioremediation Potential of *Streptomyces* sp. MOE6 for Toxic Metals and Oil

Marwa O. Elnahas<sup>1</sup>, Liyuan Hou<sup>2</sup> , Judy D. Wall<sup>3</sup> and Erica L.-W. Majumder<sup>2,\*</sup>

<sup>1</sup> Department of Chemistry of Natural and Microbial Products, Pharmaceutical Industries Research Division, National Research Centre, Cairo 12622, Egypt; marwaomar2008@yahoo.com

<sup>2</sup> Department of Chemistry, SUNY College of Environmental Science and Forestry, Syracuse, NY 13210, USA; lhou02@esf.edu

<sup>3</sup> Department of Biochemistry, University of Missouri, Columbia, MO 65211, USA; wallj@missouri.edu

\* Correspondence: emajumder@wisc.edu; Tel.: +1-315-470-6854; Fax: +1-315-470-6856

**Abstract:** Toxic metal contamination has serious effects on human health. Crude oil that may contain toxic metals and oil spills can further contaminate the environment and lead to increased exposure. This being the case, we chose to study the bio-production of inexpensive, environmentally safe materials for remediation. *Streptomyces* sp. MOE6 is a Gram-positive, filamentous bacterium from soil that produces an extracellular polysaccharide (MOE6-EPS). A one-factor-at-a-time experiments showed that the maximum production of MOE6-EPS was achieved at 35 °C, pH 6, after nine days of incubation with soluble starch and yeast extract as carbon sources and the latter as the nitrogen source. We demonstrated that MOE6-EPS has the capacity to remove toxic metals such as Co(II), Cr(VI), Cu(II) and U(VI) and from solution either by chelation and/or reduction. Additionally, the bacterium was found to produce siderophores, which contribute to the removal of metals, specifically Fe(III). Additionally, purified MOE6-EPS showed emulsifying activities against various hydrophobic substances, including olive oil, corn oil, benzene, toluene and engine oil. These results indicate that EPS from *Streptomyces* sp. MOE6 may be useful to sequester toxic metals and oil in contaminated environments.

**Keywords:** extracellular polysaccharide; heavy metal removal; *Streptomyces* sp.; bioremediation; microbially enhanced oil recovery



**Citation:** Elnahas, M.O.; Hou, L.; Wall, J.D.; Majumder, E.L.-W. Bioremediation Potential of *Streptomyces* sp. MOE6 for Toxic Metals and Oil. *Polysaccharides* **2021**, *2*, 47–68. <https://doi.org/10.3390/polysaccharides2010004>

Received: 14 December 2020

Accepted: 19 January 2021

Published: 25 January 2021

**Publisher's Note:** MDPI stays neutral with regard to jurisdictional claims in published maps and institutional affiliations.



**Copyright:** © 2021 by the authors. Licensee MDPI, Basel, Switzerland. This article is an open access article distributed under the terms and conditions of the Creative Commons Attribution (CC BY) license (<https://creativecommons.org/licenses/by/4.0/>).

## 1. Introduction

Metals, such as Zn<sup>2+</sup>, Cr<sup>3+</sup>, Hg<sup>2+</sup>, Fe<sup>2+</sup>, Fe<sup>3+</sup>, and Cu<sup>2+</sup>, are essential nutrients (with the exception of Hg<sup>2+</sup>) as they are required in trace amounts for many biological reactions. However, in high concentrations, they show serious toxicological effects in humans such as organ damage, nervous system damage, and cancer [1]. Metals and heavy metals are also used in large quantities in many production industries, including pharmaceuticals, oil refining, plastics, rubbers, and organic chemicals [2]. Improper disposal of industrial wastes and leachates often causes contamination of nearby environments and can lead to the bioaccumulation of heavy metals throughout the food chain [3]. The amount of contamination varies by site, but concentrations over 500 mg of metal ion per kg of soil or sludge have been reported for chromate [4,5]. Methods currently used to remove the toxic metals from contaminated soil, wastewater, or mixed metal-petroleum, include chemical precipitation, ion exchange, carbon adsorption, reverse osmosis, and ultra-filtration [2,6]. Disadvantages of such methods are high cost, high energy, high reagent requirements, potential for by-products to cause additional pollution, and the possible incomplete removal of the metal ions [1,7]. Thus, it is crucial to develop cost-effective and eco-friendly remediation methods for toxic metals and hydrocarbons.

Two biological methods of metal remediation are biosorption and bioaccumulation [8]. Microbial biomass from bacteria, fungi or algae has been shown to remove heavy metals

from industrial wastes and contaminated water [9]. The microorganism acts as a biosorbent, with the metals adhering to the extracellular parts of the cell or as a bioaccumulator by taking up and accumulating metals in the cell [10]. These procedures are less expensive than conventional remediation methods [11,12]. Other methods are also utilized in environmental bioremediation such as metal precipitation by microbial biopolymers, siderophores, oxidation-reduction (redox) reactions, and complexation [1,10].

Among the bacteria that have been used for metal bioremediation applications are strains belonging to the Actinobacteria [10], such as *Streptomyces* species, which are Gram-positive, filamentous bacteria [13]. Their unique growth characteristics and metabolic diversity make them good candidates for bioremediation [14]. *Streptomyces* species can represent up to 50% of soil bacterial communities, and they can also be found in fresh or saline water or hay [15,16]. Bacteria of this genus also produce bioactive secondary metabolites, which can be utilized in bioremediation applications [17].

Among the secondary metabolites produced by *Streptomyces* species are extracellular polysaccharides (EPS), carbohydrate biopolymers of different types of monosaccharide units linked by glycosidic bonds. EPS structures have the general formula of  $(C_6H_{10}O_5)_n$  where  $n$  is  $\geq 40$  and  $\leq 3000$  [18]. To provide additional functional activities, EPS can be modified with non-carbohydrate moieties such as acetate, pyruvate, and/or sulfate [19]. EPS chains are primarily linear with some having branched structures [20]. The bacterial EPS forms a protective layer around the cell that serves to limit toxic metal infiltration [3]. The ability of EPS to chelate cationic metals or metal complexes depends on the presence of negatively charged functional groups, such as uronic acid and sulfate. EPS-based metal bioremediation has advantages in cost, in lack of toxic by-products, in the potential to reuse the biopolymer and in the possible valorization of the desorbed metals or bio-mining [3,21,22]. EPS-metal remediation efficiency depends on the metal molecular size and charge density, as well as competitors for binding, the concentration of EPS and duration of the EPS-metal interaction [3].

Another environmental application for EPS is the emulsification of petroleum [23]. Conventional surfactants and emulsifiers are produced chemically; however, these synthetic molecules can be toxic and often are not easily biodegraded [24]. Research efforts have been directed to the development of natural sources for emulsifiers and surfactants with higher degradability, lower toxicity and reasonable affordability [23]. Polysaccharides have been shown to form emulsions in addition to stabilizing mixtures [25,26]. A natural emulsifier of industrial importance is xanthan gum, which is produced from *Xanthomonas campestris* and is used in many pharmaceuticals such as creams and suspensions [27]. Following the examples of other polysaccharides and xanthan gum, bacterial EPS may be functional in metal chelation and emulsification bioremediation.

Many *Streptomyces* strains also produce siderophores, another class of secondary metabolites that has potential use in bioremediation of metal-contaminated soils [28]. Siderophores are extracellular, low molecular weighted (500–1500 Da) organic chelators with high affinity and selectivity for Fe(III) [29]. These chelators are known to deliver iron from the environment to the bacterial cells or surrounding plants to overcome the shortage of available iron in oxidized soils where insoluble ferric oxides are found [29]. Even though bacteria, fungi and plants biosynthesize more than 500 known siderophore molecules, *Streptomyces* species primarily produce hydroxamates and catecholates [30,31]. Unlike the biochelation of iron, where the iron deficiency stimulates siderophore production, high concentrations of other metal cations such as copper, nickel, aluminum and cadmium lead to the stimulation of siderophore production [29,32], suggesting the potential relevance of this class of molecules in heavy metal bioremediation. Supporting this possibility was the observation that siderophores produced by *Pseudomonas fluorescens* removed Fe, Co, and Ni from uranium wastes [33]. Siderophores, then, hold promise to be an effective tool in heavy metal bioremediation.

In this study, we aimed to develop new, naturally produced bioremediation agents with lower environmental toxicity. We investigated and optimized the production and ap-

plication of *Streptomyces* sp. MOE6 siderophores and MOE6-EPS biomolecules in removing metals (Co, Cr, Cu, U, and Fe) from the surrounding aqueous solutions and determined the emulsifying ability of MOE6-EPS towards various hydrophobic phases. We demonstrated that the *Streptomyces* sp. MOE6 secondary metabolites in this study had functions and yields well suited for application as biomaterials for bioremediation activities justifying efforts to isolate related strains for development.

## 2. Materials and Methods

### 2.1. Materials and Reagents

All chemicals used were analytical grade. Galactose, lactose, mannose, xylose, and  $\text{CuSO}_4 \cdot 5\text{H}_2\text{O}$  were purchased from Sigma Chemical Co. (St. Louis, MO, USA). Dextrin, soluble starch,  $\text{CoCl}_2 \cdot 6\text{H}_2\text{O}$ , and  $\text{K}_2\text{Cr}_2\text{O}_7$  were purchased from Fisher Scientific Co. (Fair Lawn, NJ, USA). Uranyl acetate with electron microscopy grade was obtained from Electron Microscopy Science (Hatfield, PA, USA) (<https://www.emsdiasum.com/microscopy/products/chemicals/tannic.aspx#22400>). Piperazine, from Eastman Kodak (Rochester, NY, USA). Piperazine-*N,N*-bis (2-ethanesulfonic acid) (PIPES) was from Research Products International Corporation (Mount Prospect, IL, USA). All additional components, organic and inorganic, as well as solvents (benzene and toluene), were purchased from Thermo Fisher Scientific (Waltham, MA, USA).

### 2.2. Optimization for the Production of MOE6-EPS

*Streptomyces* sp. MOE6 strain was isolated from a soil sample collected from Columbia, Missouri, USA. The methods for the isolation and identification of the *Streptomyces* species were described in our previous work [34]. For the isolation of EPS, the MOE6 strain was grown in Production Medium composed of the following per liter (anhydrous  $\text{K}_2\text{HPO}_4$  3 g,  $\text{KH}_2\text{PO}_4$  1 g, NaCl 3 g, anhydrous  $\text{CaCO}_3$  0.5 g,  $\text{MgSO}_4 \cdot 7\text{H}_2\text{O}$  0.5 g, tryptone 5 g, yeast extract 5 g, glucose 10 g) pH 7.0 [35] at 30 °C for 7 days and shaken at 180 rpm. This was followed by removal of the cells by centrifugation at  $17,136 \times g$  for 20 min. The EPS was removed from cell-free culture medium by precipitation with two volumes of cold ethanol 100% *v/v*. After precipitation, the EPS was stored in ethanol at 4 °C overnight. The precipitated crude EPS was then collected by centrifugation at  $17,136 \times g$  for 20 min at 4 °C. This crude EPS was purified by redissolving in distilled water and reprecipitating with two volumes of cold 100% *v/v* ethanol. The reprecipitation step was repeated three times or until all the color was removed from the EPS and a white precipitate was obtained. Finally, the white, purified EPS precipitate was collected by centrifugation and lyophilized for further analysis.

After completion of this study, the strain was unfortunately lost. The *Streptomyces* strain MOE6 had been identified by 16S rRNA gene sequencing and comparison with those found in the National Center for Biotechnology Information (NCBI) database (5 March 2017) with accession number KY742742 (available at <https://www.ncbi.nlm.nih.gov/genbank/>). Optimization for MOE6-EPS production was performed by testing the effect of one-factor-at-a-time, i.e., in each optimization experiment, we applied the result of the former physical parameters in determining the best values for the following ones. This optimization was carried out by measuring the dry weight of lyophilized MOE6-EPS produced per liter to determine the conditions producing the maximum EPS. EPS productions were tested from cultures in 250 mL shake flasks containing 50 mL of production medium [35]. All the flasks were inoculated with 1 mL of 48 h bacterial culture.

The effects of five different incubation temperatures (25, 30, 35, 40 and 45 °C) on MOE6-EPS production were tested at pH 7 with 180 rpm shaking for 7 days of incubation. This was followed by evaluating the effect of different incubation periods and were studied over an incubation time of 10 days at 180 rpm, 35 °C, and an initial pH of 7. Moreover, the effect of various initial pHs of the culture medium on EPS production was tested over pH range of 4 to 9 (where 1N HCl and 1N NaOH were used for adjusting the initial pHs) with the

incubation shaken at 180 rpm and 35 °C and for 9 days of incubation (optimum temperature and incubation time for EPS production obtained from the previous experiments).

The effect of different carbon sources on the production of MOE6-EPS was tested with various simple and complex carbon sources (2% *w/v*) including: glucose, galactose, lactose, sucrose, mannose, xylose, soluble starch and dextrin. The glucose was omitted from the production medium when testing the effect of other sources of sugars on EPS production, while all other medium components remained the same. The experiment was carried out under the optimized conditions, i.e., at 180 rpm, 35 °C, and pH 6 over an incubation period of 9 days.

Finally, the effect of different organic and inorganic nitrogen sources (0.6% *w/v*) on the EPS production was examined, these included: yeast extract, tryptone, peptone, ammonium sulfate, sodium nitrate, sodium nitrite, as well as glycine. The tryptone and yeast extract were omitted from the production medium when testing the effect of other nitrogen sources on EPS production, and only one of the listed nitrogen sources was added to evaluate the effect of various nitrogen sources on the production. Glucose was added as a carbon source. The dry weight of cells was obtained by collecting the cells from the production medium after the incubation period, by centrifugation at  $17,136 \times g$  for 20 min and this was followed by drying the cells in an oven at 50 °C to a constant weight. The experiment was carried out under the optimized conditions, i.e., at 180 rpm, 35 °C, and pH 6 over an incubation period of 9 days.

### 2.3. Metal Removal by MOE6-EPS

The ability of MOE6-EPS to remove various metals (Co(II), Cu(II), Cr(VI), and U(VI)) from their solutions was evaluated by several colorimetric assays.

#### 2.3.1. Cobalt Removal Assay by MOE6-EPS

The ability of MOE6-EPS to chelate cobalt ions was determined by a colorimetric assay. One mL of different concentrations of purified EPS were mixed with 1 mL of a  $\text{CoCl}_2 \cdot 6\text{H}_2\text{O}$  solution (0.5 mg of  $\text{CoCl}_2 \cdot 6\text{H}_2\text{O}$ /mL) yielding final EPS concentrations of 0.125, 0.25, 0.5, 1, 2, and 4 mg/mL. After allowing the mixture to stand for five min, 0.5 mL  $\text{H}_2\text{O}_2$  of 30% *v/v* was added. This was followed by the addition of 1 mL of diethylenetriaminepentaacetic acid (DTPA) 5% *w/v*. The whole mixture was boiled for 10 min until the color was developed and measured at 530 nm [36]. To measure the concentration of cobalt chelated by MOE6-EPS, a standard curve was constructed by different concentrations of  $\text{CoCl}_2 \cdot 6\text{H}_2\text{O}$ /mL (ranging from 0.125 to 2 mg/mL).

#### 2.3.2. Chromium Reduction Assay by MOE6-EPS

We followed the method described by Method 7196A (July 1992) with some modifications to evaluate the ability of MOE6-EPS to reduce chromium as Cr(VI) in the dichromate anion to a less toxic oxidation state of Cr(III) that is much less water soluble than Cr(VI). Potassium dichromate stock solution was prepared by dissolving 141.4 mg of  $\text{K}_2\text{Cr}_2\text{O}_7$  in water and diluting it in 1 liter (where 1 mL = 50 µg of Cr). Diphenylcarbazide solution was prepared by dissolving 250 mg of 1,5-diphenylcarbazide in 50 mL acetone. For determining reduction, 1 mL  $\text{K}_2\text{Cr}_2\text{O}_7$  (3 µg of Cr) was mixed with 1-mL portions of increasing concentrations of EPS with final concentrations of 0.125, 0.25, 0.5, 1, 2, and 4 mg/mL, and the mixture was allowed to stand for five minutes. This was followed by the addition of 20 µL of stock diphenylcarbazide solution then 10 µL  $\text{H}_2\text{SO}_4$  of 10% *v/v* was added last. The whole mixture was allowed to stand for five min and the color developed was measured at 540 nm with water as a blank. The concentration of the chromium removed (either due to the reduction of Cr(VI) to Cr(III) or the removal of the dichromate anion by positive charges that might exist on the EPS) was calculated from the standard curve constructed with increasing concentrations of Cr(VI) (ranging from 0.5 to 5 µg/mL) by plotting the absorbance values (at 540 nm) against µg/mL of Cr(VI).

### 2.3.3. Copper Removal Assay by MOE6-EPS

The copper chelation capacity of MOE6-EPS was determined by the colorimetric assay described by Bermejo-Martinez and Rodriguez-Campos [37] with some modifications. Briefly, 1 mL of  $\text{CuSO}_4 \cdot 5\text{H}_2\text{O}$  solution (1.5 mg of  $\text{CuSO}_4 \cdot 5\text{H}_2\text{O}$ /mL) was mixed with increasing concentrations of EPS to yield final EPS concentrations of (0.125, 0.25, 0.5, 1, 2, and 4 mg/mL) in a final solution of volume 2 mL. After standing for 5 min, a metal chelator, 0.5 mL of 5% *w/v* diethylenetriaminepentaacetic acid (DTPA) was added. The resulting blue color was measured at 650 nm. Different concentrations of  $\text{CuSO}_4 \cdot 5\text{H}_2\text{O}$ /mL ranging from 0.25 to 4 mg of  $\text{CuSO}_4 \cdot 5\text{H}_2\text{O}$ /mL were used to construct a standard curve to measure the amount of copper chelated by EPS. The standard curve was obtained by plotting the absorbance values measured at 650 nm versus the known mg/mL of  $\text{CuSO}_4 \cdot 5\text{H}_2\text{O}$ .

### 2.3.4. Uranium Removal Assay by MOE6-EPS

For the uranium binding assay with MOE6-EPS, 100  $\mu\text{M}$  uranyl acetate ( $\text{UO}_2(\text{CH}_3\text{COO})_2$ ) stock solution was combined with EPS at final concentrations of 0.5, 1, 2, and 4 mg/mL for five min. The EPS-metal solution mixture was loaded onto a G-25 mini spin column (Sigma-Aldrich, St. Louis, MO, USA) and centrifuged for 2 min at  $28,341 \times g$ . Then 100  $\mu\text{L}$  of flow through was removed and mixed sequentially with the uranium assay reagents as follows: 100  $\mu\text{L}$  complexing solution (250 mg of trans-1,2-Diaminocyclohexane-*N,N,N,N*-tetraacetic acid monohydrate (DCTA), 50 mg of sodium fluoride, 650 mg of sulfosalicylic acid in 10 mL with a pH 7.85), 100  $\mu\text{L}$  of 20 mM Tris Buffer (pH 7.85), 500  $\mu\text{L}$  ethanol, 100  $\mu\text{L}$  of 0.05% (*w/v*) 2-(5-Bromo-2-pyridylazo)-5-(diethylamino) phenol in ethanol, and 350  $\mu\text{L}$  deionized water [38]. The mixture was incubated at room temperature for 45 min and measured spectrophotometrically at 578 nm and the concentration of the uranyl ions removed were calculated from a standard curve prepared in the same manner with a uranyl acetate range of 0–100  $\mu\text{M}$ . A negative control with EPS only and no uranyl acetate was also performed in the same manner. All experiments were conducted in triplicate, and the average values were used for further calculations.

## 2.4. Qualitative Estimation of Siderophore Produced by *Streptomyces* sp. MOE6

Siderophores are detected by the modified Chrome Azurol S (CAS) blue agar assay [39]. The CAS blue agar was prepared following the method of Schwyn and Neilands (1987) [40], with some modifications. CAS (60.5 mg) was dissolved in 50 mL distilled water and mixed with 10 mL of an iron (III) solution (1 mM of  $\text{FeCl}_3 \cdot 6\text{H}_2\text{O}$  in 10 mM of HCl). The solution (60 mL) was added slowly under stirring to a solution formed of 72.9 mg of hexadecyltrimethylammonium bromide (HDTMA) dissolved in 40 mL water. This resulted in the development of a dark blue liquid that was then autoclaved at 121 °C for 15 min. A second mixture was formed by mixing 750 mL water, 15 g agar, 30.24 g PIPES, and 12 g of a solution of 50% (*w/w*) NaOH to raise the pH to the pKa of PIPES (6.8) was also autoclaved at 121 °C for 15 min. After both solutions were autoclaved, the first solution (dye solution, while hot) was poured along the glassware wall of the container holding the molten second solution to avoid foam formation when mixed carefully. All assay glassware was pretreated with 6 M HCl to remove iron and subsequently rinsed with distilled water.

Petri dishes (10 cm in diameter) were filled with 30 mL International *Streptomyces* Project (ISP2) medium with 1.5% agar [41]. ISP2 medium was allowed to solidify and then cut into two halves. One half was removed from the plate and replaced by CAS-blue agar (15 mL). The ISP2 medium half was streaked with *Streptomyces* sp. MOE6. The streak was located far away from the borderline separating the two media. The inoculated Petri dishes were then incubated at 30 °C in the dark. Dishes were monitored daily for the inoculum growth over two weeks of incubation. The CAS reaction was determined by measuring the advance of the color-change in the CAS-blue agar (from blue to orange), starting from the borderline between the two media. Control plates of CAS-agar were prepared and incubated under the same conditions but without being inoculated with *Streptomyces* sp. MOE6.

### 2.5. Quantitative Estimation of Siderophore Produced by *Streptomyces* sp. MOE6

*Streptomyces* sp. MOE6 was allowed to grow in liquid Production Medium [35] for 7 days of incubation at 30 °C with shaking at 180 rpm. After growth, the cells were removed from the Production Medium by centrifugation at  $17,136 \times g$  for 20 min. The siderophore production by *Streptomyces* sp. MOE6 was measured with CAS as described by Schwyn and Neilands (1987) [40]. The cell-free culture medium (0.5 mL) was mixed with 0.5 mL CAS reagent (see below), then 10  $\mu$ L of CAS shuttle solution (0.2 M 5-sulfosalicylic acid) was added to accelerate the iron exchange process and the whole mixture was allowed to stand in the dark for 1 h. Finally, the absorption was measured at 630 nm.

The CAS reagent was prepared by adding 6 mL of HDTMA (10 mM) to a 100 mL volumetric flask, then 40 mL of distilled water was added. A mixture of 1.5 mL of iron III solution (1 mM of  $\text{FeCl}_3 \cdot \text{H}_2\text{O}$  dissolved in 10 mM of HCl) and 7.5 mL of 2 mM CAS stock solution were added to the diluted HDTMA in the volumetric flask slowly with stirring. Anhydrous piperazine (4.307 g) was dissolved in  $\text{H}_2\text{O}$  (30 mL) then 6.25 mL of 12 M HCl was added carefully to help dissolve the piperazine. This piperazine solution was then added to the CAS solution in the volumetric flask. The CAS reagent volume was brought to 100 mL with distilled  $\text{H}_2\text{O}$ . A standard curve was constructed with increasing amounts of the iron chelator desferrioxamine B in the range of 0 to 30  $\mu$ M. The siderophore concentrations were presented as % siderophore units (% SU) and calculated by the following equation.

$$\% \text{ Siderophore units} = (A_r - A_s) / A_r \times 100$$

where  $A_r$  = Absorbance of reference at 630 nm (Medium and CAS reagent),  $A_s$  = Absorbance of sample at 630 nm, and 100% SU = 10  $\mu$ M CAS.

### 2.6. Optimization of Siderophore Production by *Streptomyces* sp. MOE6

The effects of different physicochemical parameters on siderophore production were examined in single-factor-at-a-time experiments. The result of each optimized parameter was applied in determining the best value for the following ones. The experiment was performed in 250 mL shake flasks containing 50 mL of Production Medium [35]. All the flasks were inoculated with 1 mL of 48 h bacterial culture. The effect of different incubation temperatures (25, 30, 35, 35, 40, and 45 °C) was evaluated at pH 7 and 7 days of incubation. Additionally, the effect of different incubation times on the siderophore production was tested over 10 days of incubation pH 7 and 35 °C (optimum temperature obtained from the previous experiment). Finally, the effect of different initial pHs was examined over a pH range of 4 to 9, where the initial pH of the Production Medium was adjusted by 1N HCl or 1N NaOH, at 35 °C and for 7 days of incubation. All the culture flasks were incubated in a rotary shaker at 180 rpm.

### 2.7. Emulsifying Activities of MOE6-EPS

The emulsifying activities of MOE6-EPS were measured by a modified method of Cooper and Goldenberg (1987) [42,43]. The hydrophobic substrates were added to an aqueous phase containing various concentrations of MOE6-EPS in a ratio of 1:1 ( $v/v$ ). The mixture was agitated vigorously for 2 min and was allowed to stand for 24 h at room temperature. The hydrophobic substrates used in this study were benzene, toluene and commercial engine oil (Power Care Premium 4-cycle Engine Oil 10 W-30, Selmer, TN, USA), as well as various commercial brands of vegetable oils, including pure corn oil and pure olive oil. The emulsification index after 24 h ( $E_{24}$ ) was calculated according to the following equation [44]:

$$E_{24} = [\text{the height of emulsion layer} / \text{the overall height of the mixture}] \times 100.$$

### 3. Results

#### 3.1. Optimization of MOE6-EPS Production

For *Streptomyces* sp. MOE6, the effects of different physical parameters such as the incubation temperatures, incubation periods as well as the initial pHs were evaluated. Additionally, the effect of different carbon and nitrogen sources as nutritional requirements were tested. The results revealed that the crude MOE6-EPS production increased gradually within the tested temperature range to reach a maximum MOE6-EPS production per liter at 35 °C where the crude MOE6-EPS yield was 3.9 g/L (Figure 1a). The next parameter tested was the time of incubation required to obtain the maximum accumulated MOE6-EPS. Over 10 days of incubation at 35 °C, the crude MOE6-EPS yield increased gradually to reach the maximum production of crude MOE6-EPS (4.5 g/L) after 9 days (Figure 1b). Within the initial pH range tested (pH 4–9), the maximum production for the crude MOE6-EPS per liter was obtained at pH 6 where the yield was 5.6 g/L, whereas the minimum production of the crude MOE6-EPS was 2.0 g/L at pH 4 (Figure 1c).

The impacts of nutrient concentrations on EPS production were also evaluated. Production from equal weights of carbon sources, glucose, galactose, lactose, sucrose, mannose, xylose, dextrin and soluble starch was measured. Soluble starch showed the highest crude MOE6-EPS yield which was 11.7 g/L at 9 days, while xylose showed the minimum yield, which was 3.0 g/L (Figure 1d). These results suggest that the cells may favor consuming the longer polymers of branched carbohydrates for the production of higher amounts of MOE6-EPS compared to the simple sugars or disaccharides.

A second essential nutrient that is required by the cells for growth and EPS production is nitrogen from either organic or inorganic nitrogen compounds. The effect of six different nitrogen sources on MOE6-EPS production was evaluated in a medium lacking any other nitrogen source. The organic nitrogen sources tested in this experiment were yeast extract, tryptone, and glycine; whereas, the inorganic nitrogen sources were ammonium sulfate, sodium nitrate, and sodium nitrite. Organic nitrogen sources resulted in higher yields of MOE6-EPS compared to inorganic nitrogen sources (Figure 1e). Among the nitrogen sources tested, yeast extract or tryptone (organic nitrogen sources that also provide carbon) showed maximum crude MOE6-EPS yield per liter of 3.17 g/L and 3.1 g/L, respectively. Sodium nitrate (inorganic nitrogen source) resulted in a minimum yield of crude MOE6-EPS that was 1.2 g/L (Table 1). Collectively, then, the optimal conditions for EPS production by MOE6 are 9 days of growth at 35 °C and pH 6 with soluble starch as the carbon source and yeast extract as the nitrogen source. The results of the effect of various carbon and nitrogen sources on MOE6-EPS, as well as biomass yields, have been shown in Table 1.

**Table 1.** Nutrient impact on biomass and crude MOE6-EPS production.

Sugars	Carbon Sources (n = 3)		Sole N Source	Nitrogen Sources (n = 3)	
	Crude EPS Yield (g/L)	Biomass Yield (g/L)		Crude EPS Yield (g/L)	Biomass Yield (g/L)
Glucose	4.0 ± 0.3	1.0 ± 0.1	Tryptone	3.1 ± 0.2	1.7 ± 0.2
Galactose	3.4 ± 0.4	2.3 ± 0.3	Yeast extract	3.2 ± 0.3	2.4 ± 0.1
Mannose	3.2 ± 0.1	3.2 ± 0.2	Glycine	1.9 ± 0.2	0.8 ± <0.1
Xylose	3.1 ± 0.2	2.1 ± 0.2	NaNO <sub>3</sub>	1.2 ± <0.1	0.6 ± 0.1
Lactose	3.2 ± 0.1	2.7 ± 0.4	(NH <sub>4</sub> ) <sub>2</sub> SO <sub>4</sub>	2.3 ± 0.1	0.8 ± <0.1
Sucrose	3.4 ± 0.4	1.1 ± 0.1	NaNO <sub>2</sub>	1.3 ± <0.1	0.5 ± <0.1
Dextrin	10.0 ± 0.2	2.4 ± 0.2			
Soluble starch	11.7 ± 0.6	1.9 ± 0.1			

Concentrations of carbon and nitrogen sources in the production medium were 20 g/L and 6 g/L, respectively.

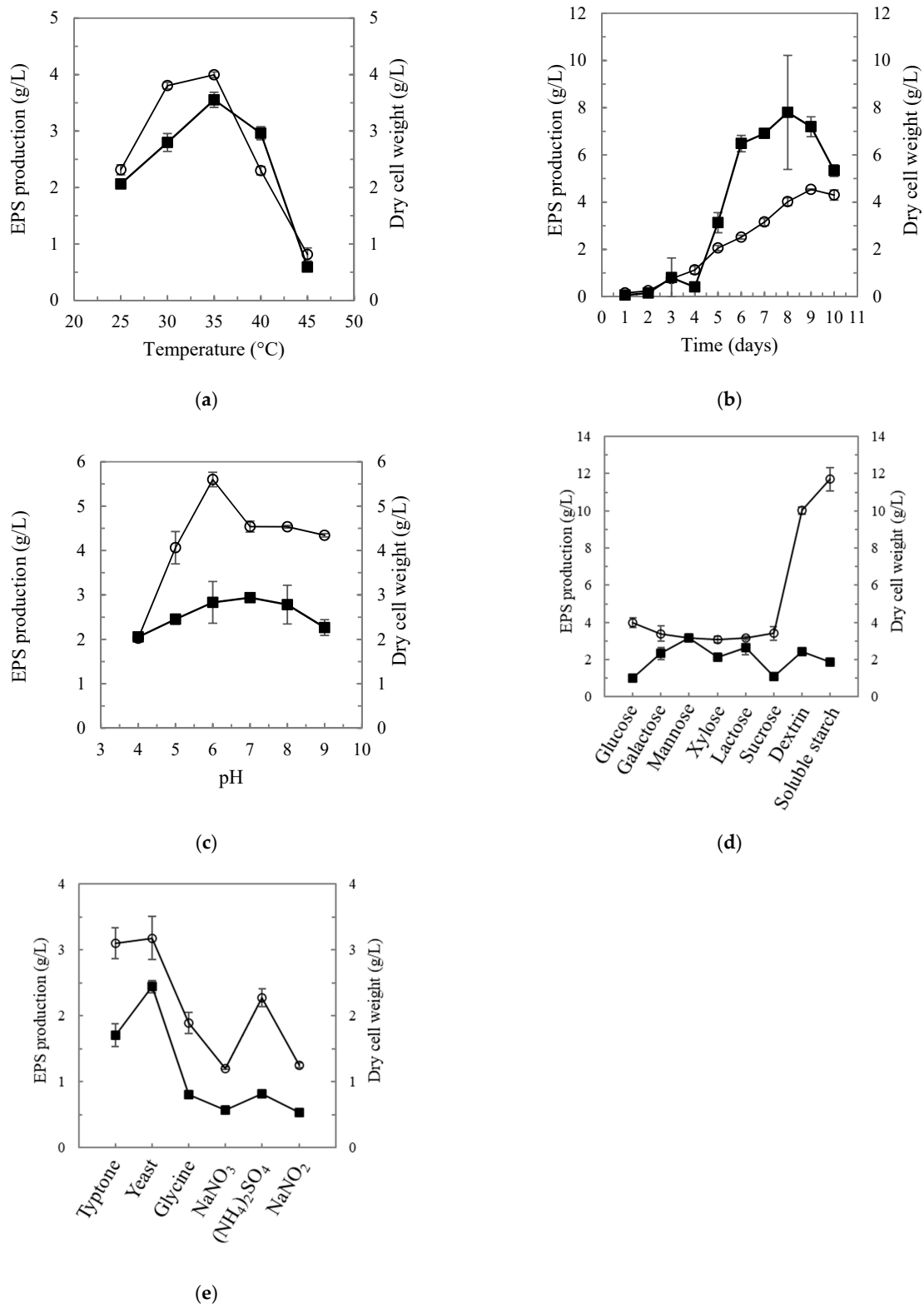


**Figure 1.** Effect of various factors on crude MOE6-EPS production. (a) Effect of different incubation temperatures, (b) effect of different incubation times, (c) effect of different initial pHs, (d) effect of different carbon sources, and (e) effect of different nitrogen sources. Triplicate samples were tested for EPS (hollow circle) and cell dry weight (solid square). Error bars were generally within the data symbol. The cultures were incubated aerobically at 180 rpm in the production medium at pH 6 and 35 °C. Triplicate samples were tested for EPS and dry weight of cells. Cells were collected by centrifugation at  $17,136 \times g$  and dried at 50 °C. Concentrations of carbon and nitrogen sources in the production medium were 20 g/L and 6 g/L, respectively.

### 3.2. Metal Sequestration by MOE6-EPS

Our previous study showed that, after the extraction, purification and lyophilization of MOE6-EPS, it appeared as a white, spongy precipitate that is water soluble, forming a viscous solution. MOE6-EPS was formed mainly of glucose, mannose and glucuronic acid. The matrix-assisted laser desorption ionization-time of flight (MALDI-TOF) analysis showed that MOE6-EPS was a low molecular weight polysaccharide with a molecular weight ranging from 8 to 16 kDa. Additionally, the chemical analysis showed that MOE6-EPS 71 ± 1% carbohydrates, 3.6 ± 0.1% uronic acid and 0.8 ± 0.1% proteins [34]. EPS polymers have been investigated as a useful tool for heavy metal remediation [3]. The negatively charged groups on EPS molecules facilitate binding to positively charged toxic metals. The ability of MOE6-EPS to chelate ferrous ions was demonstrated in our previous work and that could be attributed to the presence of the hydroxyl and carboxylic groups that were detected in the Fourier transform infrared (FTIR) spectroscopy of MOE6-EPS [34].

Here, we evaluated the ability of MOE6-EPS to chelate and presumably to remove other common contaminant metals. First, the effect of MOE6-EPS on the cobalt cations was tested with a spectrophotometric assay. The principle of this assay is that the cobalt ion is able to develop a red color when it is boiled with a metal chelator called diethylenetriamine-pentaacetic acid (DTPA) in the presence of H<sub>2</sub>O<sub>2</sub>. If another chelator (such as EPS) can compete with DTPA and is added before boiling, the color intensity formed will decrease. Increasing concentrations of MOE6-EPS were mixed with CoCl<sub>2</sub>·6H<sub>2</sub>O solution in the presence of H<sub>2</sub>O<sub>2</sub> and DTPA [36]. A decrease in the color development by DTPA after the addition of MOE6-EPS was observed. We interpret this to mean that MOE6-EPS competed with DTPA and chelated the cobalt ions. MOE6-EPS at a concentration of 0.125 mg EPS/mL chelated 15.9 ± 0.1% of the initial 123.5 µg cobalt cations/mL, and this chelation activity increased gradually with increasing MOE6-EPS concentrations, reaching 44.9 ± 0.1% chelation at 4 mg EPS/mL (Figure 2a).

Another seriously toxic metal is chromium. The removal of dichromate anions from solution by MOE6-EPS was measured with the color intensity developed during the reaction of Cr(VI) with diphenylcarbazide in an acidic medium [45]. The developed color intensity decreased gradually with increasing MOE6-EPS concentrations, indicating the removal of Cr(VI) by MOE6-EPS mediated by binding of dichromate ions or the reduction of Cr(VI) to less soluble Cr(III). The results showed that the minimum MOE6-EPS concentration used, 0.125 mg/mL, was able to remove about 1.9 ± 0.1% of the Cr(VI), while the maximum concentration used of 4 mg MOE6-EPS/mL removed 37.7 ± 0.1% of the initial amount of the dichromate (VI) (Figure 2b).

The ability of MOE6-EPS to chelate cupric ions was also evaluated by a colorimetric assay where DTPA forms a blue color with Cu<sup>2+</sup> [37]. The observed decrease in the blue color intensity is attributed to the removal of the cupric ions by MOE6-EPS due to the chelation of the Cu<sup>2+</sup>. The results showed a gradual decrease in the intensity of the generated color with increasing concentrations of the EPS. MOE6-EPS chelated 10.6 ± 0.1% of the initial amount of Cu<sup>2+</sup> cations (381.6 µg/mL) at a concentration of 0.5 mg EPS/mL, and the EPS activity to remove Cu<sup>2+</sup> increased gradually with increasing EPS concentrations to reach 24.8 ± 0.1% at a concentration of 4 mg EPS/mL (Figure 2c).

Finally, a colorimetric assay was employed to detect the ability of MOE6-EPS to remove the uranyl cations [UO<sub>2</sub>]<sup>2+</sup> from solution [38]. A decrease in the color intensity indicated the removal of the uranyl cations by MOE6-EPS, which was proportionate to the amount of MOE6-EPS added. MOE6-EPS at concentration of 4 mg/mL removed about 70 ± 0.1% of the uranyl ions from a 100 µM uranyl acetate solution (Figure 2d).

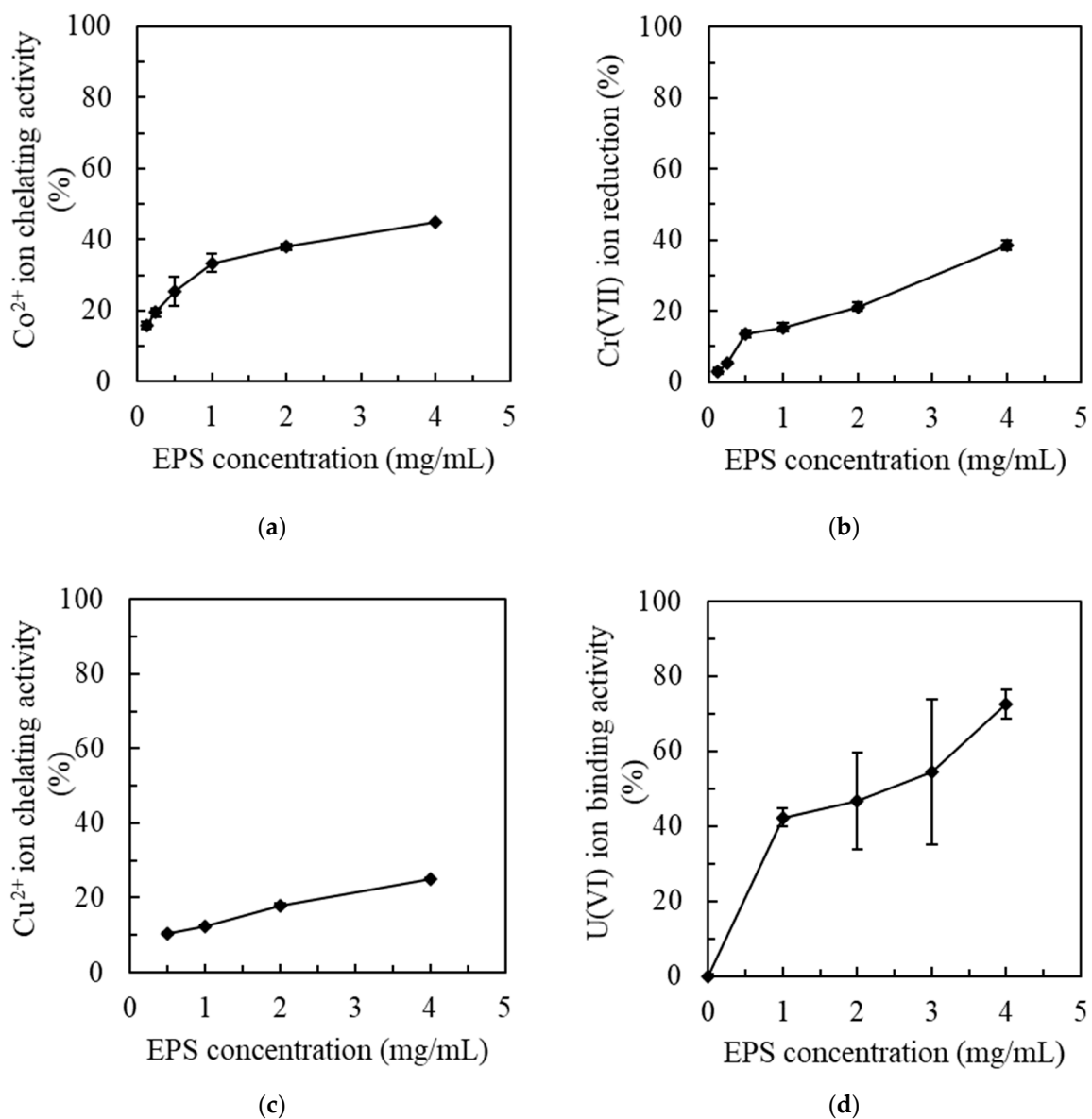


**Figure 2.** Ability of purified MOE6-EPS to remove various metals from their aqueous solutions. (a) Cobalt ion removal from aqueous solution by MOE6-EPS; 100% (*w/v*) Co<sup>2+</sup> was 123.5 µg/mL. (b) Amount of Cr(VI) in dichromate decreased by MOE6-EPS; 100% (*w/v*) Cr(VI) was 3 µg/mL. (c) Copper ion removal from aqueous solution by MOE6-EPS; 100% (*w/v*) Cu<sup>2+</sup> was 381.6 µg/mL. (d) Binding of U(VI) in uranyl ions to MOE6-EPS; 100% was 100 µM uranyl acetate. Values are means ± SD (*n* = 3).

### 3.3. Siderophores Production and Activity

#### 3.3.1. Qualitative and Quantitative Detection of Siderophores

The production of siderophores by *Streptomyces* sp. MOE6 was detected qualitatively with a modified CAS agar assay [39], following the method of Schwyn and Neilands [40]. Adding a strong chelator will remove the iron from the CAS blue dye, causing a color change from blue to orange or purple, depending on the type of siderophore secreted. Half of a Petri dish was filled with International *Streptomyces* Project (ISP2) medium with agar [41] and the other half was filled with CAS-blue agar; then, the ISP2 medium half was streaked with *Streptomyces* sp. MOE6 (Figure 3a). After incubation at 30 °C for 7 days, *Streptomyces* sp. MOE6 produced siderophores that had diffused across the Petri dish turning those portions orange, indicating the removal of the iron from the dye due to siderophore iron chelation. The orange color also suggests that the siderophore produced

was hydroxamate and not the catechol siderophores produced by other *Streptomyces* species that changes the CAS blue color into purple (Figure 3b).

The siderophore production by *Streptomyces* sp. MOE6 was also measured quantitatively. After incubating *Streptomyces* sp. MOE6 at 30 °C and 180 rpm for 7 days, the amount of the siderophore in the cell free spent medium was detected colorimetrically by the method of Schwyn and Neilands (1987), with the development of an orange color. The result showed that the amount of siderophore units was 46.1% siderophore units (=4.61  $\mu$ M CAS) after 7 days of incubation.

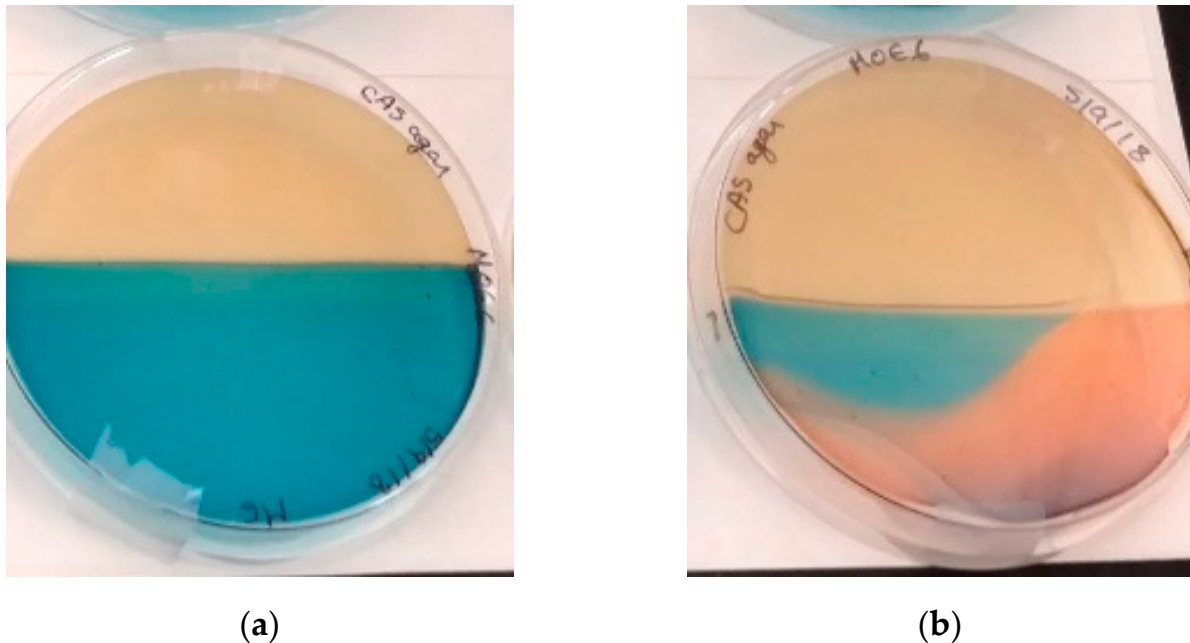


**Figure 3.** Detection of siderophores on CAS-blue agar plate with ISP2 agar medium. (a) Negative control plate “uninoculated ISP2 agar medium” and (b) ISP2 agar medium inoculated with *Streptomyces* sp. MOE6.

### 3.3.2. Siderophore Optimization

The effects of various physical culture conditions impacting the siderophore production were tested. First, the effect of different incubation temperatures (from 25 to 45 °C) was evaluated, and it was observed that the siderophore production increased gradually by increasing the temperature until obtaining the maximum production of siderophores (47.34% of siderophore units) at 35 °C and 180 rpm (Figure 4a) where 100% siderophore units equal to 10  $\mu$ M CAS. The second parameter was the incubation time required for the maximum siderophore production, and it was evaluated over 10 days of incubation at pH 7, 35 °C and 180 rpm. Within the incubation time, siderophore production increased gradually to reach the maximum production (50.6% of siderophore units) after 7 days of incubation (Figure 4b). Finally, the effect of different initial pHs of the culture medium at 35 °C and 180 rpm. The production was evaluated over a pH range (from pH 4 to pH 9). The results found that the maximum siderophore production (50.33% of siderophore units) was achieved at the neutral pH (pH 7) (Figure 4c). Our results showed that the maximum production of siderophore, which was ~50% of siderophore units (~5  $\mu$ M CAS), was achieved when the production medium was incubated at 35 °C, pH 7 and after 7 days of incubation.

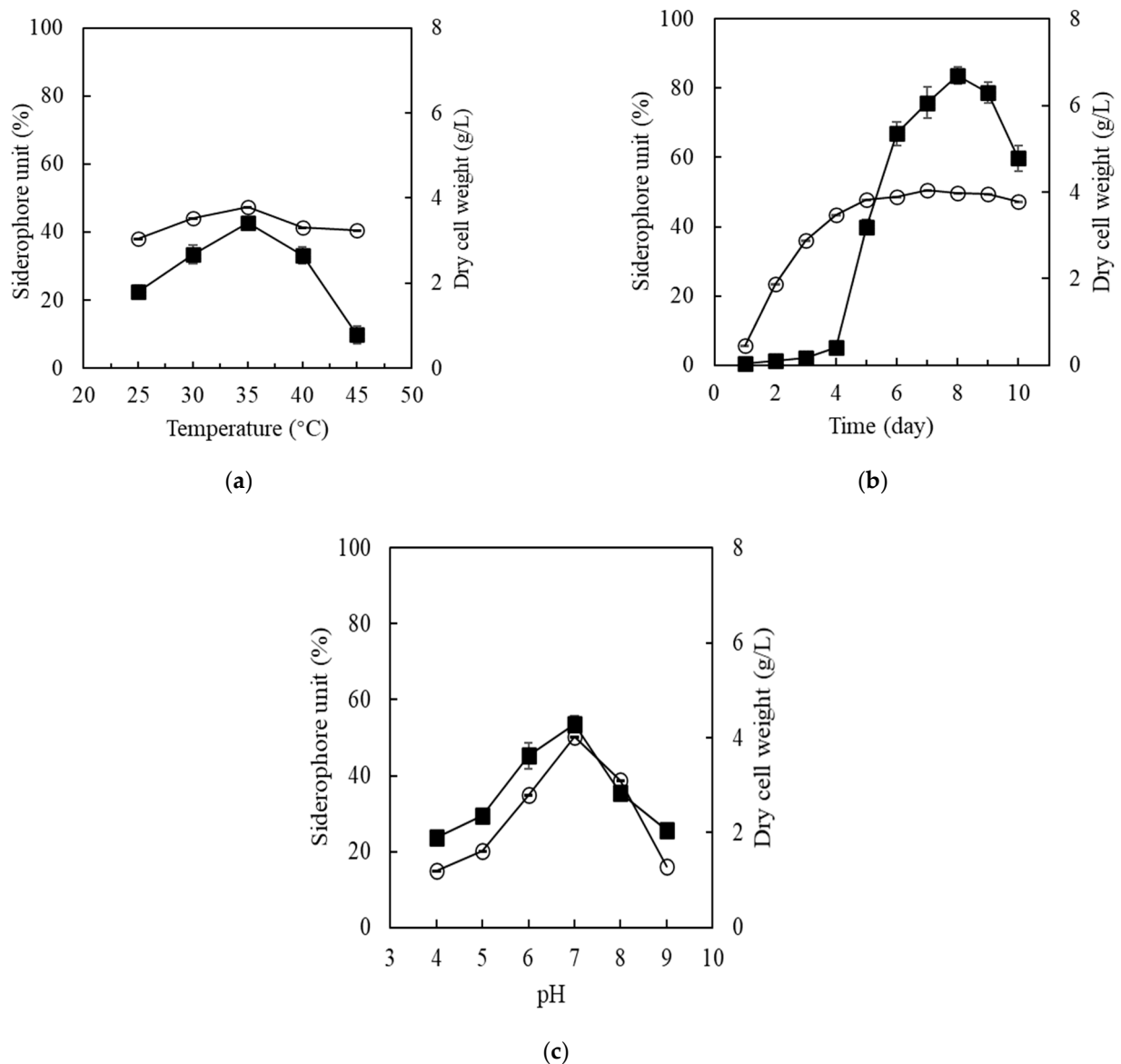


**Figure 4.** Effect of various factors on siderophore production by *Streptomyces* sp. MOE6. (a) effect of different incubation temperatures, (b) effect of different incubation times, and (c) effect of different initial pHs. Triplicate samples were tested for siderophore (hollow circle) and cell dry weight (solid square). Error bars were generally within the data symbol. The cultures were incubated aerobically at 180 rpm in production medium 35 °C if not otherwise noted. Triplicate samples were tested for EPS and dry weight of cells. Cells were collected by centrifugation at 17,136× g and dried at 50 °C. 100% siderophore unit = 10 μM CAS. Values are means ± SD ( $n = 3$ ).

### 3.4. Emulsification Activity of MOE6-EPS

Many studies have shown that microbial polysaccharides have found useful applications as emulsifying agents, resulting from the high viscosities and unique rheological properties of the microbial EPSs [46,47]. In this study, we evaluated the emulsifying activity of MOE6-EPS towards various hydrophobic phases by mixing increasing concentrations of MOE6-EPS dissolved in water with equal volumes of oils. The emulsifying index ( $E_{24}$ ) for each hydrophobic phase was calculated [42]. MOE6-EPS exhibited a noticeable emulsifying activity, as it was able to stabilize various mixtures of water and hydrophobic phases such as vegetable oils (olive oil and corn oil) and hydrocarbons (engine oil, benzene and toluene) by forming a white emulsion layer. Emulsifying activity increased gradually with increasing MOE6-EPS concentrations (Figure 5). The concentration at 4 mg EPS/mL displayed the maximum emulsification index ( $E_{24}$ ) for engine oil 89.6% and olive oil 85.6%. This was

followed by benzene at 66.4% and corn oil at 66%, whereas the lowest emulsification index was 62.4% for toluene (Figure 5).

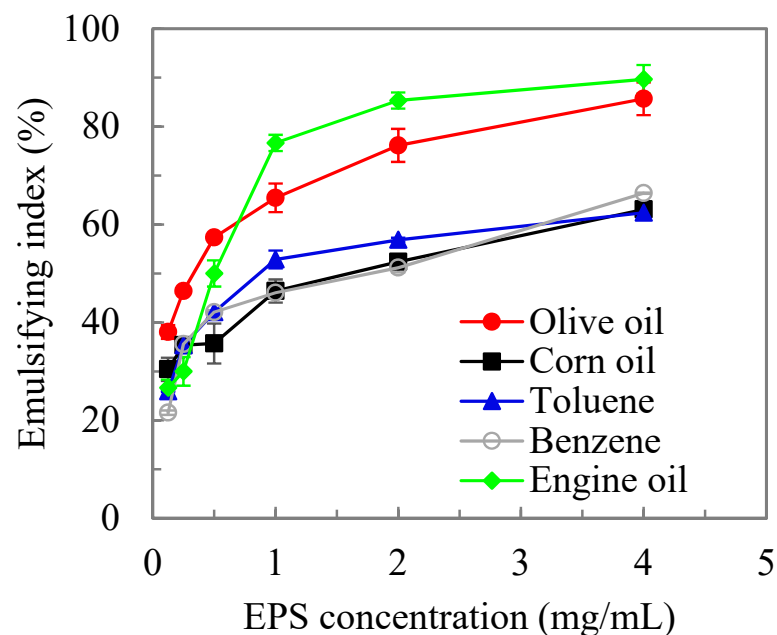


**Figure 5.** Vegetable oil/hydrocarbons-water emulsifying indices at different purified MOE6-EPS concentrations. Values were measured after mixture was left standing for 24 h at room temperature. Values are means  $\pm$  SD ( $n = 3$ ). Emulsifying index of 100% means that the emulsification layer was the full height of the entire solution.

#### 4. Discussion

In this study, several factors, including temperature, incubation time, initial pH, carbon sources, and nitrogen sources that affected the *Streptomyces* sp. MOE6 growth and crude EPS production, were investigated (Figure 1). Our results showed that an incubation time of 9 days for *Streptomyces* sp. MOE6 at 35 °C and an initial pH of 6 led to a higher yield of EPS (5.6 g/L), as compared to other conditions. Due to application of the optimal conditions obtained, this value was much higher than the 2.5 g/L reported in our previous study for MOE6 [34]. EPS production by *Streptomyces* sp. MOE6 was also higher than many other microorganisms. For instance, *Cupriavidus* sp. ISTL7 released  $3.11 \pm 0.37$  g/L EPS in Minimal salt medium (MSM) [48] supplemented with carbofuran [49]. The EPS production by *Serratia* sp.1 reached 2.45 g/L with sterile wastewater sludge as the substrate [50]. Additionally, microalgae and cyanobacteria have attracted industrial attention since they often grow quickly and release large amounts of EPS [51]. Cyanobacterium *Arthrospira platensis* generated 210 mg/L EPS after 21 days of culture [52] and EPS production of *Arthrospira* sp. was enhanced to 1.02 g/g of dry cells (about 0.7 g/L) after the two-step cultivation process [53]. These comparisons all indicated that *Streptomyces* sp. MOE6 was a promising strain that produced high yields of EPS.

The optimal temperature for *Streptomyces* sp. MOE6 to produce EPS was 35 °C (Figure 1a). The optimal growth temperature for the maximum EPS production depends on the microorganisms and the biosynthetic enzymatic activity [54]. This was in agreement with the report that states that most of *Streptomyces* sp. are mesophilic and grow in temperatures 10–37 °C [55]. Additionally, Manivasagan and coworkers [35] showed that *Streptomyces violaceus* MM72 produced the highest EPS yields and cell growth at 35 °C.

Another important factor that affects the EPS yield is the incubation time. *Streptomyces* species are well known to be relatively slow growers compared to other bacteria. The incubation time required for optimum EPS or other secondary metabolite yields varies among different species [55]. In this study, the results showed that *Streptomyces* sp. MOE6 required

nine days to achieve the optimum EPS yield (Figure 1b). These results are supported by Dezfally and Ramanayaka [56] who showed that a longer incubation time of 10 days was needed for optimum growth as well as the production of secondary metabolites from *Streptomyces flavogriseus* strain, ACTK2.

The effect of pH on the production of EPS also varies with different microorganisms [57]. In general, the optimal medium pH for EPS production ranges from 5.0 to 7.0 [54]. The optimal pH for *Streptomyces* sp. MOE6 fell within that range (Figure 1c). Moreover, the medium pH may affect the cell morphology, structure, and membrane function [58–60]. Additionally, the molecular weight distribution of EPS can be altered by culture pH [57,61]. In the study reported here, a higher EPS concentration (11.7 g/L) was attained with soluble starch as a carbon source with tryptone and yeast extract as nitrogen sources that also contain some carbon contents. Among the tested nitrogen sources, the yeast extract with glucose as the primary carbon source resulted in the highest EPS production, which was 3.2 g/L (Figure 1d,e). This may be due to different C/N ratios, which influenced the microbial metabolism and EPS production. In a study reported in 2017, the EPS productivity of *Haloferax mediterranei* decreased as C/N ratio of available substrate increased from 5 to 65 [62]. However, the high C/N ratio favors EPS production in anaerobic bioreactors for wastewater treatment [63]. Durmaz et al. found that, at a C/N ratio of 5, EPS in activated sludge had rich proteins, but fewer carbohydrates, and as the C/N ratio increased to 40, the amount of carbohydrates increased sharply [64].

Carbon sources are important factors determining the amount and the physicochemical characteristics of bacterial EPS [44]. Starch was ranked as the best substrate for extracellular polysaccharide production from *Rhodotorula minuta* ATCC 10,658 [65], as well as for *Streptomyces* sp. MOE6 in this work. Starch-industrial wastes could be applied to feed *Streptomyces* sp. MOE6 to generate MOE6-EPS, which might reduce the cost of EPS production. Thus, a high concentration of EPS could be recovered by physical (e.g., centrifugation and filtration) or chemical (e.g., ethanol precipitation and acid-base extraction) extraction methods easily allowing use as a bioflocculant and/or biosorbent [54]. Several studies have applied bioflocculants and biosorbents in wastewater treatment, metal removal, landfill leachate treatment, and soil remediation [66–68]. For instance, the polysaccharide produced by *Rhizomonas* sp. was applied to remove the humic acids from landfill leachates, a procedure that showed comparable results with conventional coagulants [66]. Additionally, the bioflocculant produced by *Pseudomonas koreensis* and *Pantoea* sp. showed significant sorption of Cd, Cr and Pb [68]. Furthermore, a previous study showed that *Pseudomonas* strain I1a and *Arthrobacter* strain D9 were functional in soil decontamination since they produced EPS that effectively retained Cd. Through the results presented here, it is clear that the strain, *Streptomyces* sp. MOE6, or its non-toxic and biodegradable EPS, showed enough potential that strains with these properties should be tested for in situ bioremediation.

We found that MOE6-EPS had the capacity to remove toxic metals such as Co(II), Cr(VI), Cu(II) and U(VI) from their aqueous solutions (Figure 2). For cations, the negatively charged carboxyl groups of uronic acid or hydroxyl groups observed in MOE6-EPS [34] likely bound metal cations on these sites. In addition, a reduction in toxicity might be achieved through the conversion of the metal to a less toxic form, which results from a chemical reduction via electron donation from EPS to an anion leading to a solubility change in the metal. Among the tested concentrations, MOE6-EPS showed the maximum chelating activity at the highest EPS concentration of 4 mg/mL. The results demonstrated that MOE6-EPS could compete with 5% (*w/v*) DTPA to chelate Co<sup>2+</sup>. This chelation could have been related to the presence of uronic acid groups, as well as the hydroxyl groups of the EPS. Four mg MOE6-EPS/mL chelated  $44.9 \pm 0.1\%$  of the initial amount of cobalt cations (123.5 µg/mL) (Figure 2a). These results were in agreement with Iyer et al. 2005 [69], who reported an EPS produced by *Enterobacter cloacae* showed the ability to chelate cobalt and this chelating activity was strongly related to the uronic acid of the EPS.

Another toxic metal of environmental concern is chromium (Cr) that exists in several oxidation states. The trivalent Cr(III) and the hexavalent Cr(VI) chromium are considered

the most common forms found in nature [70]. However, the hexavalent chromium is a human carcinogen due to its strong oxidizing potential that affects the cell structure and causes cell damage [71]. Thus, developing new low-cost methods to remove Cr(VI), either by chelation or by reducing it to Cr(III), which is a thousand times less toxic than Cr(VI), is important. Here we reported the effect of MOE6-EPS on decreasing Cr(VI) in the form of  $K_2Cr_2O_7$  from solution, monitored by a colorimetric assay which measured the reaction of Cr(VI) with diphenylcarbazid (redox indicator). The addition of EPS resulted in a diminution in the color intensity, indicating a decrease in Cr(VI). The loss of Cr(VI) suggests that the anion was either converted by chemical reduction to the less toxic and much less water soluble form Cr(III) or bound by the positive charges in the proteins that are retained with the EPS polysaccharide even after purification. The results showed that 4 mg MOE6-EPS/mL removed  $37.7 \pm 0.1\%$  of the initial amount of chromate (3  $\mu$ g) (Figure 2b). These results agreed with Harish et al. (2012) [72], who reported that an EPS isolated from *Enterobactercloacae* SUKCr1D showed the ability to reduce Cr(VI) to the less toxic Cr(III) form. As we do not have a complete chemical analysis of the MOE6-EPS, we cannot eliminate the possibility that modifications to the sugars may exist that allow binding of negatively charged species with the addition of interacting with EPS-associated proteins.

Moreover, MOE6-EPS was able to chelate  $Cu^{2+}$  ions and the effect was dose dependent. MOE6-EPS at a concentration of 4 mg/mL chelated  $25 \pm 0.1\%$  of the initial amount of  $Cu^{2+}$  cations (381.6  $\mu$ g) (Figure 2c). Similarly, a novel polysaccharide from *Bacillus firmus* was reported to chelate  $Cu^{2+}$  ions from an aqueous solution. Moreover, the results revealed that this *Bacillus* EPS contained glucuronic acid that plays an important role in metal chelation [73]. The likely mechanism of binding for the copper cations is through the negatively charged groups on the EPS binding the positively charged metal atoms.

Few studies have been reported on the removal of U(VI) from solution with bacterial EPS. Hussien et al. (2020) reported that extracellular polymeric substances extracted from *Aspergillus clavatus* had a maximum U(VI) removal efficiency of 90% at pH 5.0 with an EPS dose of 1 mg/mL [74]. Our results showed that MOE6-EPS was able to remove  $[UO_2]^{2+}$  ions from an aqueous solution (Figure 2d). This could be due to the binding or chelation of  $[UO_2]^{2+}$  ions to negatively charged groups on MOE6-EPS and/or it could be related to the reduction of U(VI) to the less soluble U(IV) by the EPS [75]. A previous study reported that the formation of a metal complex resulted from an interaction between the negative charges of a bacterial EPS and the uranyl ions [76]. The chelator in the method we used is only specific for U(VI) (U(IV) is not measured) and so we cannot determine if the uranyl ions were chelated by MOE6-EPS, reduced to insoluble U(IV) precipitates, or a combination of both. Regardless of the mechanism, MOE6-EPS showed promise for the removal of uranium.

The concentrations of toxic metals in soils vary extensively. The soils found in the Andes Mountains (Peru) are characterized by the presence of high concentrations of toxic metals. For example, the copper content ranged between 100 and 500 mg/kg and this exceeded the world average value, which is (12 mg/kg) [77]. Moreover, the soil samples collected from Gansu industrial region of the Yellow River (China) were found to be heavily contaminated with chromium (506.58 mg/kg) [5]. A soil sample that was contaminated with industrial wastewater in the Mostorud area, Egypt, showed a high concentration of cobalt that reach (146 mg/kg) [78]. Groundwater collected from two U.S. aquifers, Central Valley and High Plains showed that the concentration of naturally occurring uranium (U) exceeded 30  $\mu$ g/L, which is the maximum contaminant level determined by the U.S. Environmental Protection Agency [79]. The results reported in this study showed that MOE6-EPS was a promising candidate for the effective removal of these heavy metals from contaminated areas.

Several studies have been performed on the removal of metals by polysaccharide-based biomaterials [74,80–82] (Table 2). For instance, the biosorption capacities of nanofibrous chitin for metal ions followed the order:  $Cd^{2+}$  (330 mg/g) >  $Pb^{2+}$  (303 mg/g) >  $Cu^{2+}$  (141 mg/g) >  $Ni^{2+}$  (135 mg/g) [83]. The different biosorption capacities for various

metals may result from ionic size, atomic weight, or reduction potential of the metal and the functional groups of extracellular polymeric substances [3]. From the results obtained here, MOE6-EPS produced by *Streptomyces* sp. MOE6 had the potential to be a useful bioadsorbent. Future studies investigating the binding performance of EPS in mixed-metal solutions, aided by high resolution analytical methods, would be an important next step towards establishing EPS as a viable in-field bioremediation method.

**Table 2.** Bio-based polymers and metal ions adsorbed.

Bio-Based Polymers	Metal Ions	Maximum Biosorption Capacity (mg Metal/g Biopolymer)	Reference
Polysaccharide from <i>Bacillus firmus</i> MS-102	Pb	1103	[73]
	Cu	860	
	Zn	722	
Extracellular polymeric substances of <i>Aspergillus clavatus</i>	U(VI)	123.5	[74]
Extracellular polymeric substances of <i>Parapedobacter</i> sp. ISTM3	Cr(VI)	33.7	[80]
Extracellular polymeric substances of <i>Agrobacterium tumefaciens</i> F2	Cr(VI)	39.9	[81]
Chitin nanofibers	Ni(II)	134.7	[83]
	Zn(II)	134.0	
	Cd(II)	330.1	
	Pb(II)	303.4	
	Cu(II)	141.0	
Exopolysaccharide of <i>Paenibacillus jamilae</i>	Pb(II)	303.0	[84]
	Cu(II)	7.8	
	Zn(II)	12.3	
	Co(II)	30.1	
MOE6-EPS of <i>Streptomyces</i> sp. MOE6	Co(II)	13.8	
	Cu(II)	23.6	

Unk. indicates that the data were not provided in the article.

The processes of toxic metal desorption and polysaccharide regeneration are essential to economically viable applications and should be inexpensive [85]. Acids, alkalis, salts, various chelating agents and buffer solutions, as well as deionized water have been used for adsorbent regeneration. However, desorption of metal ions in an acidic medium is higher and more rapid than in neutral and basic media [86]. Metal desorption could be attributed to the competition between protons and metal cations. Moreover, low pH favors desorption and/or dissolution of various metal cations [87]. While the metal desorption process is considered advantageous, sometimes a loss of the biosorbent capacity has been reported, thus limiting the polysaccharide-metal biosorption activity to five cycles [88]. Desorption and regeneration of the biosorbent is necessary future studies when new EPS producing isolates are obtained.

*Streptomyces* sp. MOE6 was also found to produce siderophores. The color change response of CAS blue agar (to purple or orange) is observed with various microorganisms and this might be related to the different types of siderophores with various structures secreted by these microorganisms. There are two main groups of siderophores, hydroxamate and catechol, which resulted in highly colored complexes with Fe(III). At neutral pH, the hydroxamate forms reddish-orange or orange-colored complexes. However, the catechol resulted in reddish-purple colored complexes [40,89].

In this study, *Streptomyces* sp. MOE6 resulted in changing the blue color of CAS into an orange color, which could be related to the production of hydroxamate siderophores (Figure 3). It is well documented that *Streptomyces* and related species produce various hydroxamate siderophores [90]. For example, *Streptomyces acidiscabies* E13 produced hy-

droxamate siderophores that can bind iron and nickel [28] *Streptomyces tendae* F4 generated up to 121.2  $\mu\text{M/L}$  hydroxamate siderophores after 72 h to promote Cd uptake [91]. Correspondingly, these hydroxamate siderophores could further promote the binding of various heavy metals, including Fe(III). It was suggested that trivalent metals are more competitive for siderophore binding than divalent ones. Moreover, other non-Fe metals may compete with Fe for siderophore binding [28]. Thus, close relatives of *Streptomyces* sp. MOE6 might show a variable adsorption capacity towards different metals in treating real metal-contaminated environments.

Various culture conditions play a significant role in the siderophore production. These include incubation temperature and time, as well as initial pHs. In this study, the influence of different incubation temperatures on the production of siderophores was evaluated. *Streptomyces* MOE6 showed the maximum production of siderophores that is about 47.3% SU (=4.73  $\mu\text{M CAS}$ ) at 35 °C (Figure 4a). Previous studies on siderophore production optimization showed that two soil isolated bacterial strains (VITVK5 and VITVK6) also showed maximum production of siderophores at 35 °C [28]. Our results also revealed that the siderophore production increased gradually by increasing the incubation time to reach the highest production of 50.6% SU (5.07  $\mu\text{M CAS}$ ) after 7 days of incubation (Figure 4b). Moreover, the effect of increasing pHs (range from pH 4 to pH 9) on the siderophore production was tested. Over the test pH range *Streptomyces* MOE6 showed the maximum production of 50.3% SU (5.03  $\mu\text{M CAS}$ ) at pH7 (Figure 4c). Aerobic conditions play a critical role in the iron solubility, and in turn, the siderophore production. Fe(II) that is soluble at all physiological pHs is rapidly converted to Fe(III) in aerobic conditions and forms iron oxides that are soluble only below a pH of 3.5. Thus very small amounts of Fe(III) are available to the bacterium in oxic medium. This results in increasing siderophore production [92]. The effect of neutral pH is likely to be on the functioning of the bacterium. Lisiecki et al., 2000 [93] reported that *Enterococcus* spp. showed maximum siderophore units of 45.7% at pH 7.2 that is in a close agreement with the results in this study. Moreover, Sharma et al. 2016 [94] reported that the maximum yield of siderophore production (81.9%SU) by *Pseudomonas* species PB19 was also obtained at neutral pH (pH 7). In conclusion, the maximum production of siderophore by *Streptomyces* MOE6 was ~50% SU (=5  $\mu\text{M CAS}$ ) after an incubation time of 7 days at 35 °C and neutral pH.

MOE6-EPS also exhibited a noticeable emulsifying activity and formed consistent emulsions (>50% of emulsification index) with various vegetable oils and hydrocarbons at an EPS concentration up to 4 mg/mL (Figure 5). After 24 h more than 50% of the original emulsion volume was retained and the high emulsification index reveals the high stability of the emulsions [95]. Within the hydrocarbons we tested, the variation in emulsion indices may be explained by the lipid composition of the oils. MOE6-EPS performed better with engine oil and olive oil compared to benzene, toluene and corn oil. While benzene and toluene are hydrophobic molecules, they exist as single molecules and not bound in polymers. This would reduce the strength of the hydrophobic interactions between the EPS and the monomer aromatics, which give rise to the creation of an emulsification layer, because these interactions depend on the number of carbons and on molecule shape. While corn oil and olive oil are composed of the same classes of fatty acids and lipids, corn oil is majority polyunsaturated linoleic acid versus the monosaturated oleic acid, which is the largest fraction of olive oil [96]. The more linear shape of olive oil compared to corn oil may enhance the hydrophobic interactions with MOE6-EPS and therefore emulsification. Engine oil is reported to have longer average carbon chain lengths in the hydrocarbons than the other oils tested in this study, which would yield the most hydrophobic interactions with EPS and is consistent with having the highest MOE6-EPS emulsification index [97].

Comparing to other studies, in the present research, the emulsification index of MOE6-EPS for engine oil and olive oil was higher than that of the bioemulsifier xanthan gum and GD5EPS [98]. A previous study has reported EPS produced by *Streptococcus phocae* PI80 had strong emulsion stability against hexadecane (81.8%) [99]. *Streptomyces griseoplanus* NRRL-ISP5009 (MS1) also generated biosurfactant that showed the highest emulsification

stability of tested hydrocarbons with olive oil (71~81.1%) [100]. It is worth noting that the emulsification stability of EPS also depends on temperature, pH, and salinity [100]. For instance, the biosurfactant produced by *Streptomyces griseoplanus* NRRL-ISP 5009, SM1 was thermostable [100]. It was reported that biosurfactants from *Streptomyces* sp. SS 20 were effective in bioemulsification with stability of the emulsion from 30 to 100 °C, pH (3 to 7) and at a salt concentration of 3% (*w/v*) NaCl [101]. The wide range of pHs and temperature, and the stability at high saline conditions would enhance the application of EPS in microbial oil recovery. While MOE6-EPS showed high emulsification activity and stability, further studies are needed on similar strains to investigate the effects of pH and temperature, and salinity on the emulsification activity and emulsion particle size distribution.

Oil spills, such as the Deepwater Horizon oil spill, lead to the release of massive quantities of crude oil in natural environments, resulting in the contamination of land, air, and water [102]. Crude oil is known to contain hydrocarbons and metals (e.g., Fe, Cu, Zn, Pb, Co, Cd, and Cr) [103]. Two main strategies have been actively applied in microbial enhanced oil recovery: (1) ex-situ where desired extracellular polymeric substances were directly injected into the oil-polluted environment and (2) in-situ where functional microorganisms are injected to produce the desired extracellular polymeric substances in the oil-polluted environment [104]. Rhamnolipids from *Pseudomonas aeruginosa* [105], Lichenysin from *Bacillus licheniformis* [106], and Emulsan Glycolipopeptide from *Acinetobacter calcoaceticus* [107] have all been used in oil recovery. The emulsion from *Acinetobacter venetianus* ATCC 31,012 at 0.5 mg/mL is capable of removing 98% of crude oil absorbed to samples of limestone [108]. Most of the microorganisms applied in situ oil recovery are oil-degrading microorganisms and can release extracellular emulsifiers to facilitate microbial oil uptake and degradation [108]. Since crude oil contains various metals, it is important for the microorganisms to be tolerant of these metals [44]. In this regard, it was of interest that MOE6-EPS could bind metal cations and some anions to protect cells and ensured the function of the bacteria in the oil-polluted environment. Moreover, *Streptomyces* MOE6 produced biodegradable and low-toxicity compounds that could be generated inexhaustibly with reliable quality and quantity.

## 5. Conclusions

In conclusion, *Streptomyces* sp. MOE6 gave an environmentally relevant extracellular polysaccharide yield. One-factor-at-a-time experiments were used to identify the optimal parameters and substrates for EPS production. At the same time, MOE6-EPS showed a good capacity for removing toxic metals such as Cu(II), Co(II), U(VI), Cr(VI), and Fe(II) (Fe(II) in our previous work [34]) and for emulsifying activities against various hydrophobic phases. The results obtained in this study are important for the application of EPS in the bioremediation of metal-polluted soils or oil-polluted environments. Our observations of environmentally beneficial activities of the EPS from *Streptomyces* sp. MOE6 should stimulate additional isolation of related strains so that further studies can be made to support field trials. The metal-EPS complex stability should be explored and the competition of various toxic metals for binding to the MOE6-EPS will need to be examined. Facile desorption and regeneration of the EPS would be critical to the application of this material for the remediation of contaminated sites. Likewise, testing of these materials and strains in actual soils or marine samples in bioreactors or in the field would yield information about in situ efficacy and amount of EPS production. Taken together, these results for MOE6-EPS and other related polysaccharides suggest real potential for sustainable bioremediation strategies of complex contaminants like oil spills and industrial contamination and the need to isolate more microorganisms from these contaminated sites.

**Author Contributions:** Conceptualization, M.O.E. and E.L.-W.M.; methodology, M.O.E.; writing—original draft preparation, M.O.E. and L.H.; writing—review and editing, L.H., E.L.-W.M. and J.D.W.; visualization, L.H.; supervision, E.L.-W.M. and J.D.W. All authors have read and agreed to the published version of the manuscript.

**Funding:** This research was supported by the Egyptian Government through the Egyptian Cultural and Educational Bureau.

**Institutional Review Board Statement:** Not applicable.

**Informed Consent Statement:** Not applicable.

**Data Availability Statement:** The data presented in this study are available in the present article of Elnahas et al. (2021).

**Acknowledgments:** This research was supported by the Department of Biochemistry, University of Missouri Columbia, USA and the Research Foundation for the State University of New York.

**Conflicts of Interest:** The authors declare no conflict of interest.

## References

- Barakat, M. New trends in removing heavy metals from industrial wastewater. *Arab. J. Chem.* **2011**, *4*, 361–377. [[CrossRef](#)]
- Lakherwal, D. Adsorption of heavy metals: A review. *J. Environ. Res. Dev.* **2014**, *4*, 41–48.
- Gupta, P.; Diwan, B. Bacterial Exopolysaccharide mediated heavy metal removal: A Review on biosynthesis, mechanism and remediation strategies. *Biotechnol. Rep.* **2016**, *13*, 58–71. [[CrossRef](#)] [[PubMed](#)]
- Pan, K.; Wang, W.-X. Trace metal contamination in estuarine and coastal environments in China. *Sci. Total Environ.* **2012**, *421*, 3–16. [[CrossRef](#)] [[PubMed](#)]
- Pei, Y.; Yu, Z.; Ji, J.; Khan, A.; Li, X. Microbial community structure and function indicate the severity of chromium contamination of the Yellow River. *Front. Microbiol.* **2018**, *9*, 38. [[CrossRef](#)] [[PubMed](#)]
- Volesky, B.; Holan, Z. Biosorption of heavy metals. *Biotechnol. Prog.* **1995**, *11*, 235–250. [[CrossRef](#)] [[PubMed](#)]
- Gavrilescu, M. Removal of heavy metals from the environment by biosorption. *Eng. Life Sci.* **2004**, *4*, 219–232. [[CrossRef](#)]
- Viraraghavan, A.K.A.T. Fungal biosorption—an alternative treatment option for heavy metal bearing waste water. *Bioresour. Technol.* **1995**, *53*, 195–206. [[CrossRef](#)]
- Kapahi, M.; Sachdeva, S. Bioremediation options for heavy metal pollution. *J. Health Pollut.* **2019**, *9*, 191203. [[CrossRef](#)]
- Simeonova, A.G.T.; Ivanova, D.X. Biosorption of heavy metals by dead *Streptomyces fradiae*. *J. Environ. Eng. Sci.* **2008**, *25*, 627–632. [[CrossRef](#)]
- Hernandez, A.M.R.P.; Martinez, J.L. Metal accumulation and vanadium-induced multidrug resistance by environmental isolates of *Escherichia coli* and *Enterobacter cloacae*. *Appl. Environ. Microbiol.* **1998**, *1*, 4317–4320. [[CrossRef](#)] [[PubMed](#)]
- Knorr, D. Recovery and utilization of chitin and chitosan in food processing waste management. *Food Technol.* **1991**, *45*, 114–122.
- Hong, K.; Gao, A.-H.; Xie, Q.-Y.; Gao, H.G.; Zhuang, L.; Lin, H.-P.; Yu, H.-P.; Li, J.; Yao, X.-S.; Goodfellow, M. Actinomycetes for marine drug discovery isolated from mangrove soils and plants in China. *Mar. Drugs* **2009**, *7*, 24–44. [[CrossRef](#)] [[PubMed](#)]
- Albarracín, V.H.; Amoroso, M.J.; Abate, C.M. Isolation and characterization of indigenous copper resistant actinomycete strains. *Geochemistry* **2005**, *65*, 145–156. [[CrossRef](#)]
- Lucas, X.; Senger, C.; Erxleben, A.; Grüning, B.A.; Döring, K.; Mosch, J.; Flemming, S.; Günther, S. StreptomeDB: A resource for natural compounds isolated from *Streptomyces* species. *Nucleic Acids Res.* **2013**, *41*, D1130–D1136. [[CrossRef](#)]
- Mokrane, S.; Bouras, N.; Sabaou, N.; Mathieu, F. Actinomycetes from saline and non-saline soils of Saharan palm groves: Taxonomy, ecology and antagonistic properties. *Afr. J. Microbiol. Res.* **2013**, *7*, 2167–2178. [[CrossRef](#)]
- Schütze, E.; Klose, M.; Merten, D.; Nietzsche, S.; Senfleben, D.; Roth, M.; Kothe, E. Growth of streptomycetes in soil and their impact on bioremediation. *J. Hazard. Mater.* **2014**, *267*, 128–135. [[CrossRef](#)]
- Welman, A.D.; Maddox, I.S. Exopolysaccharides from lactic acid bacteria: Perspectives and challenges. *Trends Biotechnol.* **2003**, *21*, 269–274. [[CrossRef](#)]
- Leigh, J.A.; Coplin, D.L. Exopolysaccharides in plant-bacterial interactions. *Annu. Rev. Microbiol.* **1992**, *46*, 307–346. [[CrossRef](#)]
- Cescutti, P. Bacterial Capsular Polysaccharides and Exopolysaccharides. In *Microbial Glycobiology*; Elsevier: Amsterdam, The Netherlands, 2010; pp. 93–108. [[CrossRef](#)]
- Igiri, B.E.; Okoduwa, S.I.; Idoko, G.O.; Akabuogu, E.P.; Adeyi, A.O.; Ejiogu, I.K. Toxicity and bioremediation of heavy metals contaminated ecosystem from tannery wastewater: A review. *J. Toxicol.* **2018**, *2018*. [[CrossRef](#)]
- Wang, J.; Hu, S.; Nie, S.; Yu, Q.; Xie, M. Reviews on mechanisms of in vitro antioxidant activity of polysaccharides. *Oxidat. Med. Cell. Longev.* **2016**, *2016*. [[CrossRef](#)] [[PubMed](#)]
- Banat, I.M.; Makkar, R.S.; Cameotra, S.S. Potential commercial applications of microbial surfactants. *Appl. Microbiol. Biotechnol.* **2000**, *53*, 495–508. [[CrossRef](#)] [[PubMed](#)]
- Gutierrez, T.; Shimmield, T.; Haidon, C.; Black, K.; Green, D.H. Emulsifying and metal ion binding activity of a glycoprotein exopolymer produced by *Pseudoalteromonas* sp. strain TG12. *Appl. Environ. Microbiol.* **2008**, *74*, 4867–4876. [[CrossRef](#)] [[PubMed](#)]
- Wang, B.; Tian, H.; Xiang, D. Stabilizing the oil-in-water emulsions using the mixtures of *Dendrobium officinale* polysaccharides and gum arabic or propylene glycol alginate. *Molecules* **2020**, *25*, 759. [[CrossRef](#)]
- Zhang, R.; Belwal, T.; Li, L.; Lin, X.; Xu, Y.; Luo, Z. Recent advances in polysaccharides stabilized emulsions for encapsulation and delivery of bioactive food ingredients: A review. *Carbohydr. Polym.* **2020**, *116388*. [[CrossRef](#)]

27. Garcia-Ochoa, F.; Santos, V.; Casas, J.; Gomez, E. Xanthan gum: Production, recovery, and properties. *Biotechnol. Adv.* **2000**, *18*, 549–579. [[CrossRef](#)]
28. Schütze, E.; Ahmed, E.; Voit, A.; Klose, M.; Greyer, M.; Svatoš, A.; Merten, D.; Roth, M.; Holmström, S.J.; Kothe, E. Siderophore production by streptomycetes—Stability and alteration of ferrihydroxamates in heavy metal-contaminated soil. *Environ. Sci. Pollut. Res.* **2015**, *22*, 19376–19383. [[CrossRef](#)]
29. Dimkpa, C.O.; Svatoš, A.; Dabrowska, P.; Schmidt, A.; Boland, W.; Kothe, E. Involvement of siderophores in the reduction of metal-induced inhibition of auxin synthesis in *Streptomyces* spp. *Chemosphere* **2008**, *74*, 19–25. [[CrossRef](#)]
30. Ahmed, E.; Holmström, S.J. Siderophores in environmental research: Roles and applications. *Microb. Biotechnol.* **2014**, *7*, 196–208. [[CrossRef](#)]
31. Hider, R.C.; Kong, X. Chemistry and biology of siderophores. *Prod. Rep.* **2010**, *27*, 637–657. [[CrossRef](#)]
32. Rajkumar, M.; Ae, N.; Prasad, M.N.V.; Freitas, H. Potential of siderophore-producing bacteria for improving heavy metal phytoextraction. *Trends Biotechnol.* **2010**, *28*, 142–149. [[CrossRef](#)] [[PubMed](#)]
33. Edberg, F.; Kalinowski, B.; Holmstrom, S.J.; Holm, K. Mobilization of metals from uranium mine waste: The role of pyoverdines produced by *Pseudomonas fluorescens*. *Geobiology* **2010**, *8*, 278–292. [[CrossRef](#)] [[PubMed](#)]
34. Elnahas, M.O.; Amin, M.A.; Hussein, M.; Shanbhag, V.C.; Ali, A.E.; Wall, J.D. Isolation, characterization and bioactivities of an extracellular polysaccharide produced from *Streptomyces* sp. MOE6. *Molecules* **2017**, *22*, 1396. [[CrossRef](#)] [[PubMed](#)]
35. Manivasagan, P.; Sivasankar, P.; Venkatesan, J.; Senthilkumar, K.; Sivakumar, K.; Kim, S.K. Production and characterization of an extracellular polysaccharide from *Streptomyces violaceus* MM72. *Int. J. Biol. Macromol.* **2013**, *59*, 29–38. [[CrossRef](#)] [[PubMed](#)]
36. Flashka, H.; Barnard, A.J. *Chelates in Analytical Chemistry*; Marcel Dekker, Inc.: New York, NY, USA, 1969; Volume 5. [[CrossRef](#)]
37. Bermejo-Martinez, F.; Rodriguez-Campos, J. Photometric determination of copper with DTPA. *Microchem. J.* **1966**, *11*, 331–342. [[CrossRef](#)]
38. Johnson, D.; Florence, T. Spectrophotometric determination of uranium (VI) with 2-(5-bromo-2-pyridylazo)-5-diethylaminophenol. *Anal. Chim. Acta* **1971**, *53*, 73–79. [[CrossRef](#)]
39. Milagres, A.M.; Machuca, A.; Napoleao, D. Detection of siderophore production from several fungi and bacteria by a modification of chrome azurol S (CAS) agar plate assay. *J. Microbiol. Methods* **1999**, *37*, 1–6. [[CrossRef](#)]
40. Schwyn, B.; Neilands, J.B. Universal chemical assay for the detection and determination of siderophores. *Anal. Biochem.* **1997**, *160*, 46–56. [[CrossRef](#)]
41. El Karkouri, A.; Assou, S.A.; El Hassouni, M. Isolation and screening of actinomycetes producing antimicrobial substances from an extreme Moroccan biotope. *Pan Afr. Med. J.* **2019**, *33*. [[CrossRef](#)]
42. Cooper, D.G.; Goldenberg, B.G. Surface-active agents from two *Bacillus* species. *Appl. Environ. Microbiol.* **1987**, *53*, 224–229. [[CrossRef](#)]
43. Amodu, O.S.; Ntwampe, S.K.; Ojumu, T.V. Optimization of biosurfactant production by *Bacillus licheniformis* STK 01 grown exclusively on *Beta vulgaris* waste using response surface methodology. *BioResources* **2014**, *9*, 5045–5065. [[CrossRef](#)]
44. Ibrahim, I.M.; Konnova, S.A.; Sigida, E.N.; Lyubun, E.V.; Muratova, A.Y.; Fedonenko, Y.P.; Elbanna, K. Bioremediation potential of a halophilic *Halobacillus* sp. strain, EG1HP4QL: Exopolysaccharide production, crude oil degradation, and heavy metal tolerance. *Extremophiles* **2020**, *24*, 157–166. [[CrossRef](#)] [[PubMed](#)]
45. Method 7196A: Chromium, Hexavalent (Colorimetric), Part of Test Methods for Evaluating Solid Waste, Physical/Chemical Methods. 1992. Available online: <https://www.epa.gov/sites/production/files/2015-12/documents/7196a.pdf> (accessed on 1 August 2016).
46. Cerning, J. Exocellular polysaccharides produced by lactic acid bacteria. *FEMS Microbiol. Lett.* **1990**, *87*, 113–130. [[CrossRef](#)] [[PubMed](#)]
47. Duboc, P.; Mollet, B. Applications of exopolysaccharides in the dairy industry. *Int. Dairy J.* **2001**, *11*, 759–768. [[CrossRef](#)]
48. Rathour, R.; Gupta, J.; Tyagi, B.; Kumari, T.; Thakur, I.S. Biodegradation of pyrene in soil microcosm by *Shewanella* sp. ISTPL2, a psychrophilic, alkalophilic and halophilic bacterium. *Bioresour. Technol.* **2018**, *4*, 129–136. [[CrossRef](#)]
49. Gupta, J.; Rathour, R.; Singh, R.; Thakur, I.S. Production and characterization of extracellular polymeric substances (EPS) generated by a carbofuran degrading strain *Cupriavidus* sp. ISTL7. *Bioresour. Technol.* **2019**, *282*, 417–424. [[CrossRef](#)]
50. Bezawada, J.; Hoang, N.V.; More, T.T.; Yan, S.; Tyagi, N.; Tyagi, R.D.; Surampalli, R.Y. Production of extracellular polymeric substances (EPS) by *Serratia* sp. 1 using wastewater sludge as raw material and flocculation activity of the EPS produced. *J. Environ. Manag.* **2013**, *128*, 83–91. [[CrossRef](#)]
51. Delattre, C.; Pierre, G.; Laroche, C.; Michaud, P. Production, extraction and characterization of microalgal and cyanobacterial exopolysaccharides. *Biotechnol. Adv.* **2016**, *34*, 1159–1179. [[CrossRef](#)]
52. Trabelsi, L.; M'sakni, N.H.; Ben Ouada, H.; Bacha, H.; Roudesli, S. Partial characterization of extracellular polysaccharides produced by cyanobacterium *Arthrospira platensis*. *Biotechnol. Bioprocess Eng.* **2009**, *14*, 27–31. [[CrossRef](#)]
53. Chentir, I.; Hamdi, M.; Doumandji, A.; HadjSadok, A.; Ouada, H.B.; Nasri, M.; Jridi, M. Enhancement of extracellular polymeric substances (EPS) production in *Spirulina* (*Arthrospira* sp.) by two-step cultivation process and partial characterization of their polysaccharidic moiety. *Int. J. Biol. Macromol.* **2017**, *105*, 1412–1420. [[CrossRef](#)]
54. More, T.T.; Yadav, J.S.S.; Yan, S.; Tyagi, R.D.; Surampalli, R.Y. Extracellular polymeric substances of bacteria and their potential environmental applications. *J. Environ. Manag.* **2014**, *144*, 1–25. [[CrossRef](#)] [[PubMed](#)]
55. Hasani, A.; Kariminik, A.; Issazadeh, K. Streptomycetes: Characteristics and their antimicrobial activities. *IJABBR* **2014**, *2*, 63–75.

56. Dezfally, N.K.; Ramanayaka, J.G. Isolation, identification and evaluation of antimicrobial activity of *Streptomyces flavogriseus*, strain ACTK2 from soil sample of Kodagu, Karnataka State (India). *Jundishapur J. Microbiol.* **2015**, *8*, e15107. [[CrossRef](#)]
57. Shu, C.-H.; Lung, M.-Y. Effect of pH on the production and molecular weight distribution of exopolysaccharide by *Antrrodia camphorata* in batch cultures. *Process Biochem.* **2004**, *39*, 931–937. [[CrossRef](#)]
58. Lee, K.M.; Lee, S.Y.; Lee, H.Y. Bistage control of pH for improving exopolysaccharide production from mycelia of *Ganoderma lucidum* in an air-lift fermentor. *J. Biosci. Bioeng.* **1999**, *88*, 646–650. [[CrossRef](#)]
59. Kim, S.W.; Hwang, H.J.; Xu, C.P.; Sung, J.M.; Choi, J.W.; Yun, J.W. Optimization of submerged culture process for the production of mycelial biomass and exo-polysaccharides by *Cordyceps militaris* C738. *J. Appl. Microbiol.* **2003**, *94*, 120–126. [[CrossRef](#)]
60. Giavasis, I.; Harvey, L.M.; McNeil, B. Scleroglucan. *Biopolym. Online* **2005**. [[CrossRef](#)]
61. Lee, J.W.; Yeomans, W.G.; Allen, A.L.; Deng, F.; Gross, R.A.; Kaplan, D.L. Biosynthesis of novel exopolymers by *Aureobasidium pullulans*. *Appl. Environ. Microbiol.* **1999**, *65*, 5265–5271. [[CrossRef](#)]
62. Cui, Y.-W.; Shi, Y.-P.; Gong, X.-Y. Effects of C/N in the substrate on the simultaneous production of polyhydroxyalkanoates and extracellular polymeric substances by *Haloferax mediterranei* via kinetic model analysis. *RSC Adv.* **2017**, *7*, 18953–18961. [[CrossRef](#)]
63. Miqueleto, A.; Dolosic, C.; Pozzi, E.; Foresti, E.; Zaiat, M. Influence of carbon sources and C/N ratio on EPS production in anaerobic sequencing batch biofilm reactors for wastewater treatment. *Bioresour. Technol.* **2010**, *101*, 1324–1330. [[CrossRef](#)]
64. Durmaz, B.; Sanin, F. Effect of carbon to nitrogen ratio on the composition of microbial extracellular polymers in activated sludge. *Water Sci. Technol.* **2001**, *44*, 221–229. [[CrossRef](#)] [[PubMed](#)]
65. Samadlouie, H.R.; Jahanbin, K.; Jalali, P. Production, medium optimization, and structural characterization of an extracellular polysaccharide produced by *Rhodotorula minuta* ATCC 10658. *Food Sci. Nutr.* **2020**, *8*, 4957–4964. [[CrossRef](#)] [[PubMed](#)]
66. Zouboulis, A.I.; Chai, X.L.; Katsoyiannis, I.A. The application of biofloculant for the removal of humic acids from stabilized landfill leachates. *J. Environ. Manag.* **2004**, *70*, 35–41. [[CrossRef](#)] [[PubMed](#)]
67. Nontembiso, P.; Sekelwa, C.; Leonard, M.V.; Anthony, O.I. Assessment of biofloculant production by *Bacillus* sp. Gilbert, a marine bacterium isolated from the bottom sediment of Algoa Bay. *Mar. Drugs* **2011**, *9*, 1232–1242. [[CrossRef](#)] [[PubMed](#)]
68. Ayangbenro, A.S.; Babalola, O.O.; Aremu, O.S. Biofloculant production and heavy metal sorption by metal resistant bacterial isolates from gold mining soil. *Chemosphere* **2019**, *231*, 113–120. [[CrossRef](#)]
69. Iyer, A.; Mody, K.; Jha, B. Biosorption of heavy metals by a marine bacterium. *Mar. Pollut. Bull.* **2005**, *50*, 340–343. [[CrossRef](#)]
70. Cheung, K.; Gu, J.-D. Mechanism of hexavalent chromium detoxification by microorganisms and bioremediation application potential: A review. *Int. Biodeterior. Biodegrad.* **2007**, *59*, 8–15. [[CrossRef](#)]
71. Polti, M.A.; García, R.O.; Amoroso, M.J.; Abate, C.M. Bioremediation of chromium (VI) contaminated soil by *Streptomyces* sp. MC1. *J. Basic Microbiol.* **2009**, *49*, 285–292. [[CrossRef](#)]
72. Harish, R.; Samuel, J.; Mishra, R.; Chandrasekaran, N.; Mukherjee, A. Bio-reduction of Cr (VI) by exopolysaccharides (EPS) from indigenous bacterial species of Sukinda chromite mine, India. *Biodegradation* **2012**, *23*, 487–496. [[CrossRef](#)]
73. Salehizadeh, H.; Shojaoasadi, S. Removal of metal ions from aqueous solution by polysaccharide produced from *Bacillus firmus*. *Water Res.* **2003**, *37*, 4231–4235. [[CrossRef](#)]
74. Hussien, S.S. New studies of uranium biosorption by extracellular polymeric substances (EPSs) of *Aspergillus clavatus*, using isotherms, thermodynamics and kinetics. *Int. J. Environ. Stud.* **2020**, 1–19. [[CrossRef](#)]
75. Elsalamouny, A.R.; Desouky, O.A.; Mohamed, S.A.; Galhoum, A.A.; Guibal, E. Uranium and neodymium biosorption using novel chelating polysaccharide. *Int. J. Biol. Macromol.* **2017**, *104*, 963–968. [[CrossRef](#)]
76. Rashmi, V.; Darshana, A.; Bhuvaneshwari, T.; Saha, S.K.; Uma, L.; Prabakaran, D. Uranium adsorption and oil emulsification by extracellular polysaccharide (EPS) of a halophilic unicellular marine cyanobacterium *Synechococcus elongatus* BDU130911. *Curr. Opin. Green Sustain. Chem.* **2020**, 100051. [[CrossRef](#)]
77. Santos-Francés, F.; Martínez-Graña, A.; Alonso Rojo, P.; García Sánchez, A. Geochemical background and baseline values determination and spatial distribution of heavy metal pollution in soils of the Andes mountain range (Cajamarca-Huancavelica, Peru). *Int. J. Environ. Res. Public Health* **2017**, *14*, 859. [[CrossRef](#)] [[PubMed](#)]
78. Lotfy, S.; Mostafa, A. Phytoremediation of contaminated soil with cobalt and chromium. *J. Geochem. Explor.* **2014**, *144*, 367–373. [[CrossRef](#)]
79. Nolan, J.; Weber, K.A. Natural uranium contamination in major US aquifers linked to nitrate. *Environ. Sci. Technol. Lett.* **2015**, *2*, 215–220. [[CrossRef](#)]
80. Tyagi, B.; Gupta, B.; Thakur, I.S. Biosorption of Cr (VI) from aqueous solution by extracellular polymeric substances (EPS) produced by *Parapedobacter* sp. ISTM3 strain isolated from Mawsmi cave, Meghalaya, India. *Environ. Res.* **2020**, *191*, 110064. [[CrossRef](#)] [[PubMed](#)]
81. Pi, S.; Li, A.; Qiu, J.; Feng, L.; Zhou, L.; Zhao, H.-P.; Ma, F. Enhanced recovery of hexavalent chromium by remodeling extracellular polymeric substances through engineering *Agrobacterium tumefaciens* F2. *J. Clean. Prod.* **2021**, *279*, 123829. [[CrossRef](#)]
82. Na, Y.; Lee, J.; Lee, S.H.; Kumar, P.; Kim, J.H.; Patel, R. Removal of heavy metals by polysaccharide: A review. *Polym.-Plast. Technol. Mater.* **2020**, *59*, 1–21. [[CrossRef](#)]
83. Liu, D.; Zhu, Y.; Li, Z.; Tian, D.; Chen, L.; Chen, P. Chitin nanofibrils for rapid and efficient removal of metal ions from water system. *Carbohydr. Polym.* **2013**, *98*, 483–489. [[CrossRef](#)]
84. Pérez, J.A.M.; García-Ribera, R.; Quesada, T.; Aguilera, M.; Ramos-Cormenzana, A.; Monteoliva-Sánchez, M. Biosorption of heavy metals by the exopolysaccharide produced by *Paenibacillus jamilae*. *World J. Microb. Biotechnol.* **2008**, *24*, 2699. [[CrossRef](#)]

85. Ali, I. New generation adsorbents for water treatment. *Chem. Rev.* **2012**, *112*, 5073–5091. [[CrossRef](#)] [[PubMed](#)]
86. Srivastava, S.; Goyal, P. Reusability of Biomaterial: A Cost-effective Approach. In *Novel Biomaterials*; Springer: Berlin/Heidelberg, Germany, 2010; pp. 93–96. [[CrossRef](#)]
87. Zhou, Y.-F.; Haynes, R.J. A comparison of inorganic solid wastes as adsorbents of heavy metal cations in aqueous solution and their capacity for desorption and regeneration. *Water Air Soil Pollut.* **2011**, *218*, 457–470. [[CrossRef](#)]
88. Kanamarlapudi, S.; Chintalpudi, V.K.; Muddada, S. Application of biosorption for removal of heavy metals from wastewater. *Biosorption* **2018**, *18*, 69. [[CrossRef](#)]
89. Payne, S.M. Detection, isolation, and characterization of siderophores. In *Method Enzymology*; Elsevier: Amsterdam, The Netherlands, 1994; Volume 235, pp. 329–344. [[CrossRef](#)]
90. Cruz-Morales, P.; Ramos-Aboites, H.E.; Licona-Cassani, C.; Selem-Mójica, N.; Mejía-Ponce, P.M.; Souza-Saldívar, V.; Barona-Gómez, F. Actinobacteria phylogenomics, selective isolation from an iron oligotrophic environment and siderophore functional characterization, unveil new desferrioxamine traits. *FEMS Microbiol. Ecol.* **2017**, *93*, fix086. [[CrossRef](#)] [[PubMed](#)]
91. Dimkpa, C.O.; Merten, D.; Svatos, A.; Büchel, G.; Kothe, E. Siderophores mediate reduced and increased uptake of cadmium by *Streptomyces tendae* F4 and sunflower (*Helianthus annuus*), respectively. *J. Appl. Microbiol.* **2009**, *107*, 1687–1696. [[CrossRef](#)] [[PubMed](#)]
92. Winkelmann, G. Ecology of siderophores with special reference to the fungi. *Biometals* **2007**, *20*, 379. [[CrossRef](#)] [[PubMed](#)]
93. Lisiecki, P.; Wysocki, P.; Mikucki, J. Occurrence of siderophores in enterococci. *Zent. Bakteriolog.* **2000**, *289*, 807–815. [[CrossRef](#)]
94. Sharma, T.; Kumar, N.; Rai, N. Production and optimization of siderophore producing *Pseudomonas* species isolated from Tarai region of Uttarakhand. *Int. J. Pharm. Biol. Sci.* **2016**, *7*, 306–314.
95. Sacco, L.P.; Castellane, T.C.L.; Polachini, T.C.; de Macedo Lemos, E.G.; Alves, L.M.C. Exopolysaccharides produced by *Pandoraea* shows emulsifying and anti-biofilm activities. *J. Polym. Res.* **2019**, *26*, 91. [[CrossRef](#)]
96. Gunstone, F.D. *Fatty acid and Lipid Chemistry*; Springer: Berlin/Heidelberg, Germany, 2012. Available online: <https://www.springer.com/gp/book/9780751402537> (accessed on 5 January 2020).
97. O'Connor, R.T.; Herb, S. Specifications of fatty acid composition for identification of fats and oils by gas liquid chromatography. *J. Am. Oil Chem. Soc.* **1970**, *47*, 186A–195A. [[CrossRef](#)]
98. Vinothini, G.; Latha, S.; Arulmozhi, M.; Dhanasekaran, D. Statistical optimization, physio-chemical and bio-functional attributes of a novel exopolysaccharide from probiotic *Streptomyces griseorubens* GD5. *Int. J. Biol. Macromol.* **2019**, *134*, 575–587. [[CrossRef](#)] [[PubMed](#)]
99. Kanmani, P.; Satish kumar, R.; Yuvaraj, N.; Paari, K.A.; Pattukumar, V.; Arul, V. Production and purification of a novel exopolysaccharide from lactic acid bacterium *Streptococcus phocae* PI80 and its functional characteristics activity in vitro. *Bioresour. Technol.* **2011**, *102*, 4827–4833. [[CrossRef](#)] [[PubMed](#)]
100. Elkhawaga, M.A. Optimization and characterization of biosurfactant from *Streptomyces griseoplanus* NRRL-ISP5009 (MS1). *J. Appl. Microbiol.* **2018**, *124*, 691–707. [[CrossRef](#)] [[PubMed](#)]
101. Hayder, N.; Alaa, S.; Alsalm, H. Optimized Conditions for bioemulsifier production by local *Streptomyces* sp. SS 20 isolated from hydrocarbon contaminated soil. *Rom. Biotechnol. Lett.* **2014**, *19*, 8979–8993.
102. Gutierrez, T.; Berry, D.; Yang, T.; Mishamandani, S.; McKay, L.; Teske, A.; Aitken, M.D. Role of bacterial exopolysaccharides (EPS) in the fate of the oil released during the deepwater horizon oil spill. *PLoS ONE* **2013**, *8*, e67717. [[CrossRef](#)]
103. Vane, C.H.; Kim, A.W.; Moss-Hayes, V.; Turner, G.; Mills, K.; Chenery, S.R.; Barlow, T.S.; Kemp, A.C.; Engelhart, S.E.; Hill, T.D.; et al. Organic pollutants, heavy metals and toxicity in oil spill impacted salt marsh sediment cores, Staten Island, New York City, USA. *Mar. Pollut. Bull.* **2020**, *151*, 110721. [[CrossRef](#)]
104. Fan, Y.; Wang, J.; Gao, C.; Zhang, Y.; Du, W. A novel exopolysaccharide-producing and long-chain n-alkane degrading bacterium *Bacillus licheniformis* strain DM-1 with potential application for in-situ enhanced oil recovery. *Sci. Rep.* **2020**, *10*, 8519. [[CrossRef](#)]
105. Amani, H.; Müller, M.M.; Sylđatk, C.; Hausmann, R. Production of microbial rhamnolipid by *Pseudomonas Aeruginosa* MM1011 for ex situ enhanced oil recovery. *Appl. Biochem. Biotechnol.* **2013**, *170*, 1080–1093. [[CrossRef](#)]
106. Qiu, Y.; Xiao, F.; Wei, X.; Wen, Z.; Chen, S. Improvement of lichenysin production in *Bacillus licheniformis* by replacement of native promoter of lichenysin biosynthesis operon and medium optimization. *Appl. Microbiol. Biotechnol.* **2014**, *98*, 8895–8903. [[CrossRef](#)]
107. Chamanrokh, P.; Assadi, M.M.; Noohi, A.; Yahyai, S. Emulsan analysis produced by locally isolated bacteria and *Acinetobacter calcoaceticus* RAG-1. *J. Environ. Health Sci. Eng.* **2008**, *5*, 101–108.
108. Karlapudi, A.P.; Venkateswarulu, T.C.; Tammineedi, J.; Kanumuri, L.; Ravuru, B.K.; Dirisala, V.r.; Kodali, V.P. Role of biosurfactants in bioremediation of oil pollution—A review. *Petroleum* **2018**, *4*, 241–249. [[CrossRef](#)]